BIOCHEMISTRY
including biophysical chemistry & molecular biology
Article

Biochemistry **2011,** *50,* 1567–1581 1567
DOI: 10.1021/bi101504w

Dithiothreitol Causes HIV-1 Integrase Dimer Dissociation While Agents Interacting With the Integrase Dimer Interface Promote Dimer Formation

Manuel Tsiang,* Gregg S. Jones, Magdeleine Hung, Dharmaraj Samuel, Nikolai Novikov, Susmith Mukund, Katherine M. Brendza, Anita Niedziela-Majka, Debi Jin, Xiaohong Liu, Michael Mitchell, Roman Sakowicz, and Romas Geleziunas

Gilead Sciences, 333 Lakeside Drive, Foster City, California 94404, United States

Received September 15, 2010; Revised Manuscript Received January 10, 2011

ABSTRACT: We have developed a homogeneous time-resolved fluorescence resonance energy transfer (FRET)-based assay that detects the formation of HIV-1 integrase (IN) dimers. The assay utilizes IN monomers that express two different epitope tags that are recognized by their respective antibodies, coupled to distinct fluorophores. Surprisingly, we found that dithiothreitol (DTT), a reducing agent essential for in vitro enzymatic activity of IN, weakened the interaction between IN monomers. This effect of DTT on IN is dependent on its thiol groups, since the related chemical threitol, which contains hydroxyls in place of thiols, had no effect on IN dimer formation. By studying mutants of IN, we determined that cysteines in IN appear to be dispensable for the dimer dissociation effect of DTT. Peptides derived from the IN binding domain (IBD) of lens epithelium derived growth factor/transcriptional coactivator p75 (LEDGF), a cellular cofactor that interacts with the IN dimer interface, were tested in this IN dimerization assay. These peptides, which compete with LEDGF for binding to IN, displayed an intriguing equilibrium binding dose−response curve characterized by a plateau rising to a peak, then descending to a second plateau. Mathematical modeling of this binding system revealed that these LEDGF-derived peptides promote IN dimerization and block subunit exchange between IN dimers. This dose−response behavior was also observed with a small molecule that interacts with the IN dimer interface and inhibits LEDGF binding to IN. In conclusion, this novel IN dimerization assay revealed that peptide and small molecule inhibitors of the IN−LEDGF interaction also stabilize IN dimers and promote their formation.

HIV-1 integrase (IN) catalyzes the insertion of viral DNA into the host genome in two reaction steps (*1*). In the first step referred to as 3′-processing, IN removes a dinucleotide from both ends of the viral double-stranded DNA. During the second step referred to as 3′-end joining, IN catalyzes the concerted integration of both 3′-processed ends of the viral DNA into host DNA. IN prepares the host DNA by producing staggered cleavage sites on both strands which are separated by five base pairs. The integration process is then completed with the repair of the gaps at the integration junctions by host enzymes. During the process of HIV-1 infection, IN is bound to viral DNA and is transported to the nucleus as part of a large nucleoprotein assemblage called the preintegration complex (PIC) (*2*−*7*). In addition to IN, the PIC contains other viral (*6*, *8*) and cellular factors (*5*, *7*, *9*−*17*).

HIV-1 IN is organized into three domains. The N-terminal domain (NTD) (amino acids 1−50) contains a zinc-binding motif (*18*, *19*) and contributes to IN multimerization. The NTD is necessary for full catalytic activity (*20*, *21*). The catalytic core domain (CCD) (amino acids 51−212) contains three acidic amino acids (D64, D116, E152) termed the catalytic triad which coordinate divalent metal ions at the active site (*22*, *23*). The C-terminal domain (CTD) (amino acids 213−288), which is the least conserved domain between retroviral INs, binds the viral DNA ends (specifically at the LTR) and is also involved in multimerization of IN (*24*, *25*).

*To whom correspondence should be addressed. E-mail: MTsiang@gilead.com. Phone: (650) 522-5860. Fax: (650) 522-5143.

In vitro, HIV-1 IN forms an equilibrium mixture of monomers, dimers, tetramers, and higher-order oligomers in the absence of DNA. The relative ratio of these species can be affected by enzyme concentration, detergent, and zinc ions (*20*, *21*, *25*−*27*). During the process of infection, IN engages the host factor LEDGF which helps tether IN to the host chromatin (*14*−*17*, *28*).

LEDGF binds HIV-1 IN through an evolutionarily conserved domain (amino acids 347−429) in the C-terminal region termed the IN binding domain (IBD) (*29*, *30*). The IBD is both necessary and sufficient for the interaction of LEDGF with HIV-1 IN. The solution structure and cocrystal structure of IBD with the HIV-1 IN CCD, HIV-2 two-domain IN (NTD + CCD) and maedi-visna virus (MVV) two-domain IN (NTD + CCD) have been reported (*31*−*34*). The IBD binds to a small pocket at the IN CCD dimer interface. The amino acids of IN involved in the interaction with IBD have been validated by site-directed mutagenesis studies (*31*, *35*−*37*) and through selection of resistant viruses capable of replication in cells overexpressing the IBD (*38*). The interaction between full-length IN and LEDGF also involves residues at the NTD, first revealed by mutagenesis studies (*15*) and recently confirmed by the cocrystal structure of IN NTD + CCD with IBD (*33*). LEDGF and IBD can promote detectable IN tetramer formation at IN concentrations of 1−14 μM (*39*, *40*). It was proposed that the IN tetramer has two low affinity and two high affinity binding sites for the IBD of LEDGF (*40*). LEDGF appears to be important for HIV-1 integration and replication since siRNA-mediated knock-down of LEDGF or overexpression

Published on Web 01/11/2011

of the IBD of LEDGF impairs these functions (*38*, *41*−*43*). On the basis of these observations, the IN−LEDGF interaction represents a potential target for antiviral intervention (*44*−*48*), which has recently been validated by the discovery of small molecule inhibitors of the IN−LEDGF interaction that also possess HIV-1 antiviral activity (*49*).

Using a homogeneous time-resolved Förster resonance energy transfer (FRET)-based assay and mathematical modeling, we have previously determined the very high affinity of the IN monomer−monomer interaction with a dimer dissociation constant, K_{dimer} of ~70 pM and that in a 10 nM solution, ~89% of IN was in dimeric form (*48*). Our most recent studies using this IN dimerization assay have revealed that the reducing agents DTT and β-mercaptoethanol (β-ME) weaken the IN monomer−monomer interaction. Using additional mathematical modeling in our data analysis, we discovered that competitors of the IN−LEDGF interaction which bind to the IN dimer interface, also promote IN dimerization and block IN subunit exchange. We also showed that this novel system can be used to measure the on- and off-rate constants of competitors of LEDGF binding to IN dimers.

EXPERIMENTAL PROCEDURES

Peptides and Reagents. All the peptides used in this study were custom synthesized and purified (> 90% purity) by Anaspec Inc. (San Jose, CA). Dithiothreitol (catalog no. 43816), β-mercaptoethanol (catalog no. M6250), threitol (catalog no. 263559), ethylene glycol (catalog no. 293237), and tetraphenylarsonium chloride (catalog no. T2,530-5) were all purchased from Sigma-Aldrich (St. Louis, MO).

Proteins. Expression vectors and methods for expression and purification of 6His-IN, IN-Flag, 6His-INCCD(F185K), and LEDGF-Flag proteins have been previously described (*48*). The four cysteines of IN: C56, C65, C130, and C280 were mutated to serines to generate 6His-IN(4Ser) and IN(4Ser)-Flag using the QuikChange Multi Site-Directed Mutagenesis kit (catalog no. 200531, Agilent Technologies, La Jolla, CA). Both 6His-IN(4Ser) and IN(4Ser)-Flag were purified using the same protocols as their respective wild-type counterparts (*48*). INCCD(F185K)-Flag was constructed by fusing INCCD(F185K) to an N-terminal 8His sequence which is cleavable by the rTEV protease and to a C-terminal GSG-Flag sequence. The cloning primers were NdeINCore5p: 5′-TTTCATATGCATGGACAAGTAGACTG3′ and H3INCoreGSGFlag3p: 5′-TTTAAGCTTTCATTTGTCATCATCGTCTTTGTAGTCACCGCTGCCTTCTTTAGTTTGTATGTCTGTTG-3′. After amplification of the INCCD(F185K) sequence with these primers, the PCR product was purified using the QIAquick PCR Purification Kit (catalog no. 28104, QIAGEN, Valencia, CA) and digested with NdeI and *Hin*dIII. The digested PCR product was purified on a 1% agarose gel and cloned into the NdeI and *Hin*dIII sites of a modified version of the pET28a vector which carries an 8His sequence and an rTEV protease recognition sequence (catalog no. 69864, EMD BioSciences, La Jolla, CA). The resulting construct was pET28-N8H-rTEV-CCD(F185K)-GSGFlag. Protein was produced in *Escherichia coli* BL21-(DE3) (catalog #C6000−03, Invitrogen, Carlsbad, CA). Methods for purification of 8His-rTEV-INCCD(F185K)-Flag and subsequent protease cleavage to release the INCCD(F185K)-Flag were similar to those used for 8His-rTEV-IN-Flag and have been previously described (*48*).

Competition Binding Assay for the IN-LEDGF Interaction. This is a homogeneous time-resolved FRET (HTRF) assay that measures the interaction of HIV-1 IN (N-terminal 6His-tag) and LEDGF (C-terminal Flag-tag) in the presence of a competitor of LEDGF (*48*).

Equilibrium End Point Assay for IN−IN Association. This assay measures the interaction of two IN monomers to form a dimer using a homogeneous time-resolved FRET format and has been previously described (*48*). Briefly, N-terminally 6His-tagged IN (6His-IN) and C-terminally Flag-tagged IN (IN-Flag) were mixed and allowed to reach equilibrium in the presence of anti-6His-XL665 and anti-Flag-EuCryptate antibodies (catalog no. 61HISXLA and no. 61FG2KLA, Cisbio-US, Inc., Bedford, MA) for 6 h. The HTRF signal is not only generated by the formation of 6His-IN-IN-Flag heterodimers through the interaction of free 6His-IN and IN-Flag monomers, but also through subunit exchange between 6His-IN and IN-Flag dimers as they temporarily dissociate into monomers. For dose−response studies, agents were added immediately after 6His-IN and IN-Flag were mixed (each at a final concentration of 10 nM). For agents that promote IN dimerization, dose−response curves were analyzed with eq II to determine the EC_{50} and the IC_{50} components. The DTT and β-ME dose−response curves were analyzed with eq III to determine the IC_{50}.

Kinetic Assay for IN−IN Association. For the kinetic assay of IN−IN association, the buffer conditions were the same as in the equilibrium end point assay, except that the two binding partners (27.3 nM each) and a test agent were first preincubated separately with the antibody conjugates (i.e., 0.45 nM Anti-Flag-EuCryptate and 10 nM Anti-6His-XL665) for 1 h at room temperature. Kinetic measurement was started after addition of 20 μL of a test agent and 27.5 μL of one binding partner to 27.5 μL of the other binding partner. After combination of the two binding partners and the test agent, the concentrations of antibody conjugates remained the same, but the concentration of each binding partner was reduced to 10 nM. In contrast to the equilibrium end point measurement, the kinetic measurement was performed in the absence of 100 mM KF. The time course of 6His-IN and IN-Flag association was analyzed by direct curve fitting using eq I represented by Scheme A. Typically, a control time course (without test agent) was run simultaneously with a time course in the presence of a test agent. The concentration of the test agent was carefully chosen to capture any alteration of the time course relative to the control with no test agent. The time course without the test agent was analyzed first by curve fitting to the sum of FRET signal generating species (i.e., IN heterodimer species $S \times (AB + ABL + ABL_2)$ where S represents a conversion factor of the 665 nm/620 nm ratio into nM) to determine the on- and off-rate constants of IN monomer−monomer interaction (i.e., k_1 and k_{-1}). The time course with test agent, possessing the same k_1 and k_{-1}, was then analyzed in the same way to determine the on- and off-rate constants of the test agent (i.e., k_2 and k_{-2}) but only if the test agent promoted IN dimerization.

Binding Model for IN−IN Interaction in the Presence of an IN Dimer Ligand. By modifying the model for IN−IN interaction we described previously (*48*) to incorporate an agent that binds to the IN dimer interface (Scheme A), it was possible to model the dose−response of 6His-IN-IN-Flag heterodimer formation in the presence of varying concentrations of such a dimer ligand, L. Only one sequence of dimer binding reaction by L is shown. The remaining three sequences are similar and are

represented by "..." in Scheme A. Under this scenario, the sum ($AB + ABL + ABL_2$) is detectable by HTRF and can be monitored. For simplicity, we assume that the dissociation constant of the dimer ligand L from the IN dimer is $K_d = k_{-2}/k_2 = k_{-3}/k_3$.

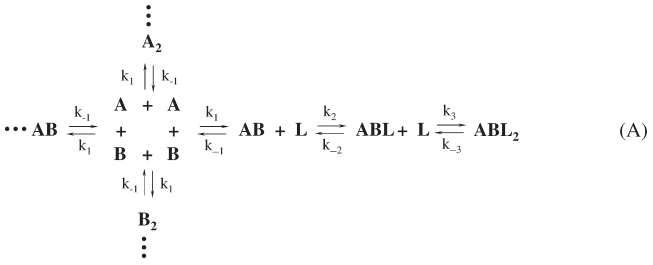

(A)

Scheme A can be written as a system of 12 differential eqs I.

$$\frac{dA}{dt} = 2k_{-1}A_2 + k_{-1}AB - k_1\left(\frac{A}{2}\right)\left(\frac{B}{4}\right) - k_1\left(\frac{A}{2}\right)\left(\frac{A}{4}\right)$$

$$\frac{dB}{dt} = 2k_{-1}B_2 + k_{-1}AB - k_1\left(\frac{A}{4}\right)\left(\frac{B}{2}\right) - k_1\left(\frac{B}{2}\right)\left(\frac{B}{4}\right)$$

$$\frac{dA_2}{dt} = k_1\left(\frac{A}{4}\right)\left(\frac{A}{4}\right) - k_{-1}A_2 - k_2A_2\left(\frac{L}{4}\right) + k_{-2}A_2L$$

$$\frac{dB_2}{dt} = k_1\left(\frac{B}{4}\right)\left(\frac{B}{4}\right) - k_{-1}B_2 - k_2B_2\left(\frac{L}{4}\right) + k_{-2}B_2L$$

$$\frac{dAB}{dt} = k_1\left(\frac{A}{2}\right)\left(\frac{B}{4}\right) - k_{-1}AB - k_2AB\left(\frac{L}{2}\right) + k_{-2}ABL$$

$$\frac{dL}{dt} = \left(k_{-2}ABL - k_2AB\left(\frac{L}{2}\right) - k_3ABL\left(\frac{L}{2}\right) + k_{-3}ABL_2\right) + \left(k_{-2}A_2L - k_2A_2\left(\frac{L}{4}\right) - k_3A_2L\left(\frac{L}{4}\right) + k_{-3}A_2L_2\right) + \left(k_{-2}B_2L - k_2B_2\left(\frac{L}{4}\right) - k_3B_2L\left(\frac{L}{4}\right) + k_{-3}B_2L_2\right)$$

$$\frac{dABL}{dt} = k_2AB\left(\frac{L}{2}\right) - k_{-2}ABL - k_3ABL\left(\frac{L}{2}\right) + k_{-3}ABL_2$$

$$\frac{dA_2L}{dt} = k_2A_2\left(\frac{L}{4}\right) - k_{-2}A_2L - k_3A_2L\left(\frac{L}{4}\right) + k_{-3}A_2L_2$$

$$\frac{dB_2L}{dt} = k_2B_2\left(\frac{L}{4}\right) - k_{-2}B_2L - k_3B_2L\left(\frac{L}{4}\right) + k_{-3}B_2L_2$$

$$\frac{dABL_2}{dt} = k_3ABL\left(\frac{L}{2}\right) - k_{-3}ABL_2$$

$$\frac{dA_2L_2}{dt} = k_3A_2L\left(\frac{L}{4}\right) - k_{-3}A_2L_2$$

$$\frac{dB_2L_2}{dt} = k_3B_2L\left(\frac{L}{4}\right) - k_{-3}B_2L_2 \qquad \text{(I)}$$

The dimer ligand dose−response of the sum ($AB + ABL + ABL_2$) describes a curve that rises from a plateau to a peak followed by a decline to a second plateau below the initial plateau when $L = 0$. This dose−response can be phenomenologically analyzed by eq II:

$$y = \left[M - \frac{(M-S)EC_{50}{}^n}{EC_{50}{}^n + x^n}\right] - \left[K - \frac{K \times IC_{50}{}^m}{IC_{50}{}^m + x^m}\right] \qquad \text{(II)}$$

where y = % binding, x = concentration of dimer ligand L, S = 100 = the start of the plateau, $(M - K)$ = the end of the second plateau, EC_{50} = concentration at half-maximal rise and IC_{50} = concentration at half-maximal decline, n = Hill coefficient of the EC_{50} component, m = Hill coefficient of the IC_{50} component. The DTT and β-ME dose−response curves were analyzed with eq III after conversion of the data to % control to determine the 50% inhibitory concentration, IC_{50}.

$$y = \frac{100 \times IC_{50}{}^n}{IC_{50}{}^n + [I]^n} \qquad \text{(III)}$$

where y = % control, n = Hill coefficient, and [I] = DTT or β-ME concentration.

RESULTS

DTT Alters the Competition Binding Dose−Response of Inhibitors of the IN−LEDGF Interaction. Since dithiothreitol (DTT) is necessary to observe IN enzymatic activity in vitro (strand transfer reaction), we tested DTT in an HTRF-based IN−LEDGF interaction assay (*48*). DTT was added to a dose−response performed with a peptide derived from LEDGF (amino acids 354−378) that competes with LEDGF binding to IN. Unexpectedly, inclusion of 2 mM DTT appeared to enhance the FRET signal for a range of LEDGF(354−378) competitor peptide concentrations by introducing a peak into the dose−response and causing the curve to shift toward the right (Figure 1A,C). This alteration of the competition dose−response is independent of the competitor used as it was observed with other LEDGF-derived peptides and tetraphenyl arsonium chloride (TPArCl), a small molecule competitor (Figure 1B,D). Because of this alteration of the dose response curve, DTT was omitted from our standard IN−LEDGF interaction assay. On the basis of the competition binding model for the IN−LEDGF interaction that was previously described (*48*), the appearance of the dose−response curves in the presence of DTT suggested a weakening of the IN monomer−monomer interaction. These previous simulations revealed that at a fixed K_i for a LEDGF competitor with increasing values of IN K_{dimer} (i.e., decreasing affinity between IN monomers), the roughly sigmoidal shape of the competition dose−response curve at low values of K_{dimer} gradually lifted to a peak that became more pronounced with increasing values of K_{dimer} (Figure 3B in ref *48*). The ascending phase of the peak is mediated by a shift toward more IN dimer formation when relatively low concentrations of the competitor occupied on the average one of two binding sites on newly formed IN dimers, allowing additional LEDGF to bind to the remaining site and thus increasing the signal. At higher competitor concentrations, competitor binding to IN is no longer primarily realized through new dimer formation but through displacement of LEDGF, resulting in the descending phase. A very tight IN monomer−monomer interaction leaves virtually no monomers to be promoted to dimers by the competitor, resulting in the absence of a peak in the dose response curve, whereas weaker IN monomer−monomer interactions allowed more monomers to be present initially and to be shifted to dimers by the addition of the competitor, resulting in the peak in the dose−response curve, indicative of a weakened monomer−monomer interaction.

The curves shown in Figure 1A,B were replotted using the raw data without normalization (Figure 1C,D). The data show that addition of 2 mM DTT decreased the baseline signal by 18−21%. To assess the effect of DTT on the formation of the IN−LEDGF complex, a DTT dose−response was performed using the same HTRF-based IN−LEDGF interaction assay (Figure 1E). At 2 mM DTT, the level of IN−LEDGF complex was reduced by ~22%, which is in agreement with the reduction observed in Figure 1C,D.

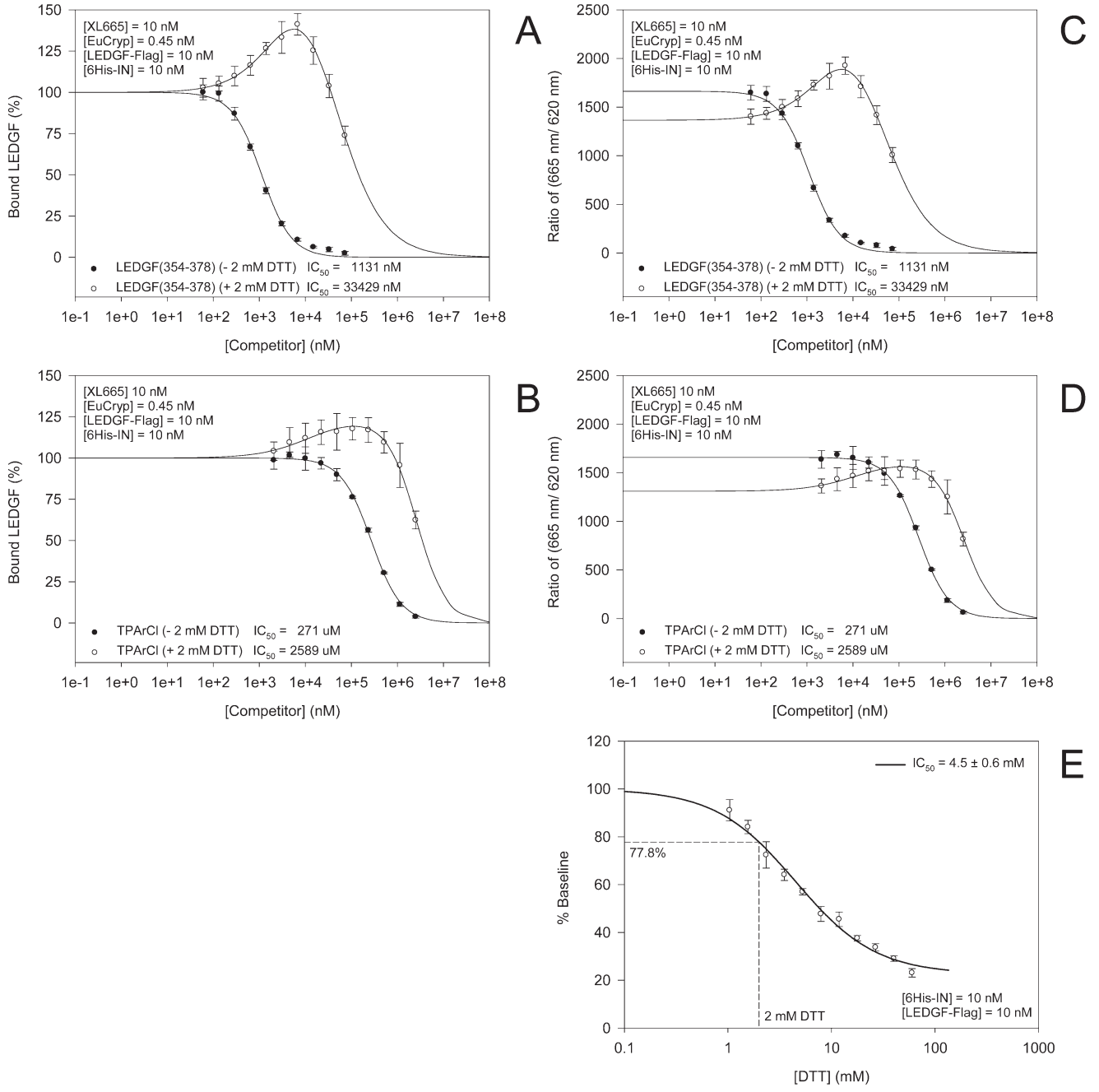

FIGURE 1: Effect of DTT on competition dose−response using the IN−LEDGF HTRF assay. (A) Competition dose−response of the LEDGF derived peptide, LEDGF (354−378) in the absence and presence of 2 mM DTT. (B) Competition dose−response of a small molecule tetraphenyl arsonium chloride (TPAsCl) in the absence and presence of 2 mM DTT. (C) Same as panel A, where the data were plotted as the raw ratio of (665 nm/620 nm). (D) Same as panel B, where the data were plotted as the raw ratio of (665 nm/620 nm). For both panels A and B, the data represent the mean of quadruplicate runs with standard deviations shown as error bars. The data are expressed as a percentage relative to the level of IN bound LEDGF in the absence of competitor. (E) Effect of DTT on IN−LEDGF Interaction. The data represent the mean of quadruplicate runs with standard deviations shown as error bars. The data are expressed as a percentage relative to the baseline representing the level of IN−LEDGF complex in the absence of DTT. See also a simulation of the effect of increasing IN dimer dissociation constant K_{dimer} on the level of IN heterodimer [AB] and IN bound LEDGF in Figure S1, Supporting Information.

DTT and β-ME Weaken IN Monomer−Monomer Interaction. To determine whether DTT promotes dissociation of IN dimers, it was tested in an HTRF-based IN dimerization assay (Figure 2A). DTT decreased the HTRF signal generated by the interaction of the 6His-IN/IN-Flag pair in a dose-dependent manner with an IC_{50} of 2.2 mM while showing no effect on the 6His-AQ-Flag control peptide which is flanked by 6His and Flag epitope tags. This result suggested that the DTT-mediated signal decrease in the IN dimerization assay was not due to dissociation of antibodies from the 6His and/or Flag tags (Figure 2A). When β-mercaptoethanol (β-ME), which is structurally equivalent to half a molecule of DTT, was tested in the IN dimerization assay, a similar effect was observed though the IC_{50} was 48 mM (Figure 2B). These results show that DTT and β-ME are capable of weakening the IN monomer−monomer interaction.

The Thiol Groups in DTT and β-ME Are Required for the Weakening of IN Monomer−Monomer Interactions. To test whether the weakening effect of DTT and β-ME on the interaction of IN monomers is dependent on the thiol groups in these molecules, we tested threitol and ethylene glycol, which are

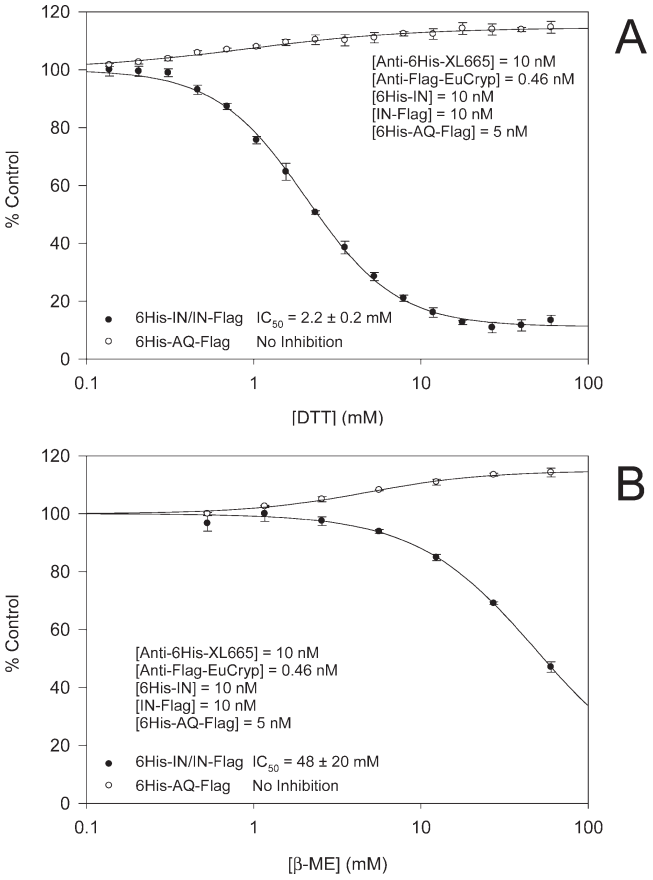

FIGURE 2: Effect of DTT and β-ME on IN dimerization. (A) DTT dose−response. (B) β-ME dose−response. The dose−response was performed using an HTRF-based assay with either 6His-IN and IN-Flag to assess the effect on the formation of IN heterodimers (closed circles) or with 6His-AQ-Flag, a peptide with an N-terminal 6His tag and a C-terminal Flag tag to assess the effect on antibody conjugate binding to these tags (open circles). For both panels A and B, the data represent the mean of quadruplicate runs with standard deviations shown as error bars. The data are expressed as a percentage relative to the control representing the level of IN dimers in the absence of DTT or β-ME.

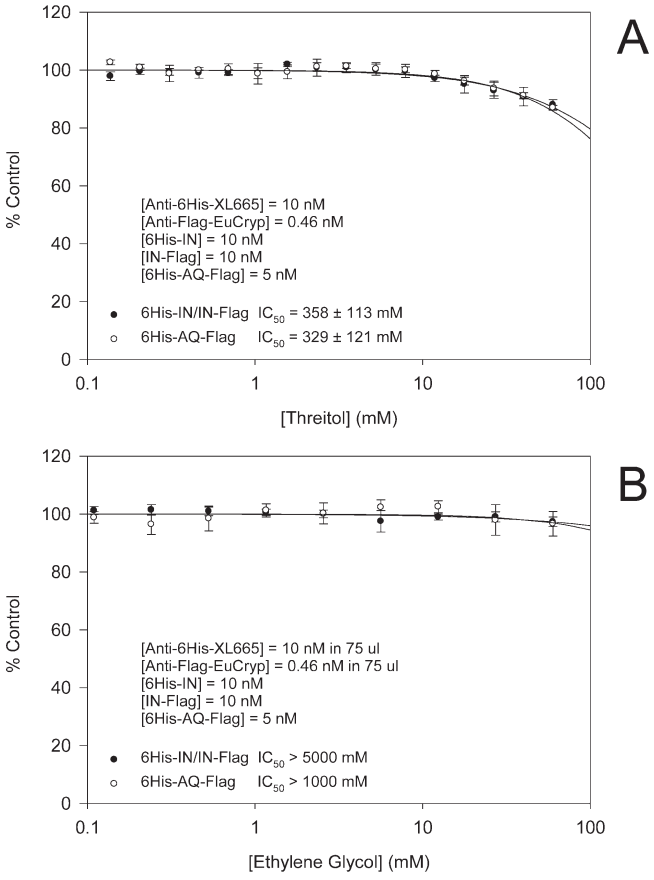

FIGURE 3: Effect of threitol and ethylene glycol on IN dimerization. (A) Threitol dose−response. (B) Ethylene glycol dose−response. The dose response was performed using an HTRF based assay with either 6His-IN and IN-Flag to assess the effect on the formation of IN heterodimers (closed circles) or with 6His-AQ-Flag, a peptide with an N-terminal 6His tag and a C-terminal flag tag to assess the effect on antibody conjugate binding to these tags (open circles). For both panels A and B, the data represent the mean of quadruplicate runs with standard deviations shown as error bars. The data are expressed as a percentage relative to the control representing the level of IN dimers in the absence of DTT or β-ME.

analogues of DTT and β-ME respectively in which the thiol groups have been replaced by hydroxyl groups (Figure 3). Neither threitol nor ethylene glycol weakened the IN monomer−monomer interaction suggesting that the effect of DTT and β-ME on IN dimer formation is mediated by their thiol groups.

Cysteines in IN Are Dispensable for DTT-Mediated Weakening of IN Dimers. We hypothesized that the thiol groups of DTT or β-ME could react with the thiol groups of cysteines on IN, forming transient adducts that weakened the monomer−monomer interaction. To test this idea, we mutated four of six cysteines in IN (C56, C65, C130, and C280) to serines in both the 6His-tagged and the Flag-tagged IN constructs. The resulting mutant IN proteins were named 6His-IN(4Ser) and IN(4Ser)-Flag. The two remaining cysteines (C40 and C43) located in the N-terminal domain were not altered since they are necessary for the formation of a zinc finger domain (*20*). Both 6His-IN(4Ser) and IN(4Ser)-Flag were capable of binding to LEDGF with affinities similar to wild-type 6His-IN (data not shown). Testing these mutants for strand-transfer activity confirmed previous observations that serine substitutions at 56, 65, 130, and 280 did not affect in vitro enzymatic activities (data not shown) (*50*, *51*). In addition, the K_{dimer} for the mutant pair of INs was comparable to that of the WT pair (55.6 pM vs 72.6 pM, see Figure 4A,B). These results suggest that the structures of the two mutant INs were not grossly altered.

Both the wild-type and the mutant pair of INs were tested in the IN heterodimer formation assay with increasing concentrations of DTT or β-ME. The susceptibility of the mutant IN pair to DTT and β-ME was not affected when compared to the wild-type pair (Table 1). To assess the effect of DTT and β-ME on the rate constants of the IN monomer−monomer interaction, we performed the time course of 6His-IN-IN-Flag heterodimer formation either in the absence of additive or in the presence DTT or β-ME (Figure 4). Both DTT (2 mM) and β-ME (40 mM) decreased the on-rate constant k_1 and increased the off-rate constant k_{-1} of the wild-type IN pair, resulting in a 19-fold and 22-fold increase in K_{dimer}, respectively (Figure 4A). The effect of DTT and β-ME on the dimerization rate constants of the mutant IN pair was similar to those of the wild-type IN pair. A decrease of the on-rate constant k_1 and an increase of the off-rate constant k_{-1} were again observed, resulting in a 22-fold and 25-fold increase in K_{dimer} in the presence of 2 mM DTT and 40 mM β-ME, respectively (Figure 4B). Taken together, these results suggest that these four cysteines (C56, C65, C130, and C280) in IN are not required for the dissociation of IN dimers by DTT or β-ME.

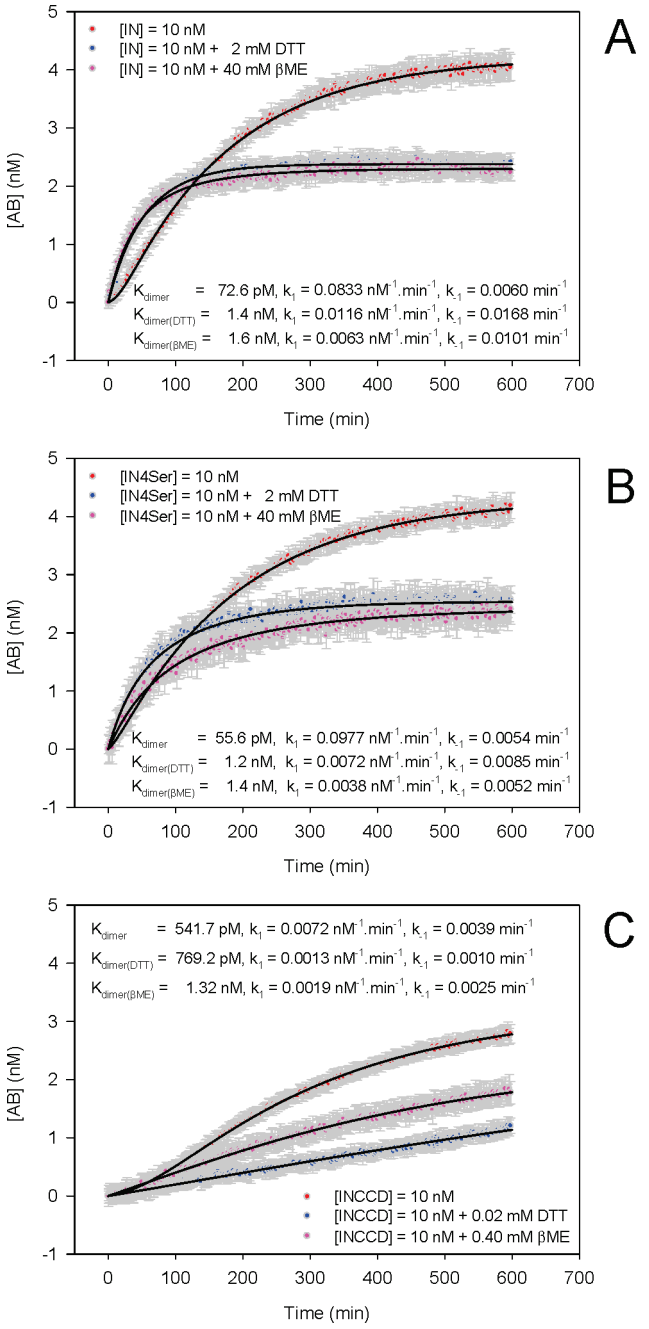

FIGURE 4: Effect of DTT and β-ME on the kinetics of IN−IN association. (A) Kinetics of wild-type 6His-IN and IN-flag association. (B) Kinetics of mutant 6His-IN(4Ser) and IN(4Ser)-flag association. (C) Kinetics of 6His-INCCD and INCCD-flag association. Ten nanomolar each of 6His-IN (or 6His-IN(4Ser) or 6His-INCCD) and IN-Flag (or IN(4Ser)-Flag or INCCD-Flag) pre-equilibrated with both antibody conjugates in the absence (red circles) or presence of DTT (blue circles) or β-ME (magenta circles) were mixed and FRET signal generation was measured for 600 min. The time course was analyzed using Scheme A and eq I where $[A]_o + [A_2]_o = 10$ nM, $[B]_o + [B_2]_o = 10$ nM and $[L]_o = 0$ nM. The on-rate constant (k_1) and off-rate constant (k_{-1}) were determined by curve fitting using eq I. For panels A, B, and C, the data represent the mean of dodecaplicate runs with standard deviations shown as error bars. The data are expressed as the concentration of IN heterodimer AB in nM.

Deletion of the NTD and CTD of IN Increases Susceptibility to DTT-Mediated Disruption of IN Dimers. To assess whether the NTD which contains the two remaining cysteines (C40 and C43) and the CTD are required for IN dimer susceptibility to DTT and β-ME, we tested the catalytic core domain (CCD) of IN in the IN dimerization assay. Specifically, the 6His-INCCD(F185K) and INCCD(F185K)-Flag pair was tested for IN heterodimer formation with increasing concentrations of DTT or β-ME. The F185K substitution is commonly engineered into IN to increase its solubility (*25*). Although this mutation has been shown to decrease tetramer formation (*40*), it preserves in vitro catalytic activity (*25*) and is located distally to the dimerization interface; thus it is not anticipated that the F185K substitution would affect IN dimerization which is the focus of this study. We hypothesized that if cysteines 40 and 43 located in the NTD were the targets of DTT, then the INCCD dimer which lacks the NTD should be refractory to the disrupting effect of DTT. Our results showed that INCCD is even more susceptible to both DTT and β-ME when compared to IN or IN(4Ser), with IC_{50} values of ~0.03 and 0.3 mM, respectively (Table 1). Next, we tested the effect of DTT and β-ME on the rate constants of monomer−monomer interaction using the INCCD pair. The results showed that while INCCD has a K_{dimer} of 541.7 pM, about 7.5-fold greater than that of full-length IN, it is 70-fold and 138-fold more susceptible to DTT and β-ME than full-length IN. Because the INCCD dimer displays greater susceptibility to DTT and β-ME, we needed to lower the concentrations of these two reducing agents to measure on-rate and off-rate constants for the INCCD pair. We thus tested DTT and β-ME at 100-fold lower concentrations to assess their effect on the rate constants of INCCD. DTT at 0.02 mM decreased the on-rate constant k_1 to a greater extent than it did to the off-rate constant k_{-1}, resulting in a ~1.42-fold increase (equivalent to ~142-fold increase if 2 mM DTT were used) in K_{dimer}. β-ME at 0.4 mM behaved similarly by decreasing both on- and off-rate constants, resulting in a ~2.44-fold increase (equivalent to ~244-fold increase if 40 mM DTT were used) in the value of K_{dimer} (Figure 4C). These increases of 142-fold and 244-fold when corrected for the 7.5-fold lower intrinsic affinity between monomers of INCCD become 19-fold and 33-fold, respectively, which is very similar to the fold-increases observed for 2 mM DTT and 40 mM β-ME with wild-type and 4Ser INs. These results showed that the NTD and CTD do not confer susceptibility to DTT but instead appear to mitigate this susceptibility in the full-length enzyme.

Table 1: Dimer Disruption Potency of Various Agents in the IN Dimerization Assay

	IN-IN	IN(4Ser)-IN(4Ser)	INCCD−INCCD	6His-AQ-flag[c]
reagent	IC_{50} (mM)	IC_{50} (mM)	IC_{50} (mM)	IC_{50} (mM)
dithiothreitol	2.2	2.0	0.032	> 400
dithioerythritol[a]	2.5			> 400
threitol	> 350			> 330
2,2′-thiodiethanol	> 500			
1-thioglycerol	42			> 400
2-mercaptoethanol	36	34	0.26	> 400
ethylene glycol	> 5000			> 1000
1,2-ethanedithiol	1.5			> 400
ethanol	> 500			
TCEP·HCl[b]	0.7			17
acetonitrile	1800			1200

[a]Diastereoisomer of dithiothreitol. [b]Tris-(2-carboxyethyl)phosphine hydrochloride, an odorless reducing agent for protein applications. [c]A peptide containing an N-terminal 6His-tag connected to a C-terminal Flag-tag via an α-helical linker made of 6 (AQ) repeats. It is used as a control to assess the effect of reagents on anti-6His and anti-Flag antibody conjugate binding.

Reducing Agents with Thiols Dissociate IN Dimer in a Manner Distinct from Solvation. In an effort to understand the underlying mechanism of IN dimer dissociation by DTT or β-ME, we tested additional thiol-containing and nonthiol-containing reagents for their ability to dissociate IN dimers (Table 1). We previously noted that the dissociating activity is related to the presence of thiol groups, as threitol and ethylene glycol, analogues of DTT and β-ME lacking the thiol group are inactive in the same concentration range. Our data also revealed (Table 1) that the IN dimer dissociating activity of an agent is related to the number of thiol groups, with agents containing two thiol groups (DTT, dithioerythritol, 1,2-ethanedithiol) being ~10−20-fold more active than agents containing only one thiol group (β-ME, 1-Thioglycerol). In addition, the effect of DTT does not appear to be stereospecific since dithioerythritol, a diastereoisomer of DTT is equally active. In contrast, an agent with a non-nucleophilic sulfur atom (2,2′-thiodiethanol) is unable to disrupt IN dimers. TCEP hydrochloride, a non-thiol-containing reducing agent, has activity comparable to that of DTT against 6His-IN-IN-Flag (IC_{50} = 0.7 mM), but it can also cause dissociation of anti-6His and anti-Flag antibodies from their epitopes (IC_{50} = 17 mM) which complicates interpretation of the effect on IN dimers (Table 1). Finally, acetonitrile, a polar solvent which was previously reported to dissociate the RT heterodimer (IC_{50} = 8% or 1390 mM) by solvation (*52*), is ineffective at dissociating IN dimers relative to thiol-containing agents (Table 1). In conclusion, reducing agents with thiol groups seem most effective at disrupting HIV-1 IN dimers.

LEDGF-Derived Peptides That Compete with LEDGF Binding to IN Promote IN Dimerization. We previously demonstrated that LEDGF-derived peptides were able to compete with LEDGF binding to IN using an HTRF-based assay (*48*). Next, we wanted to determine if such peptides that interact with the LEDGF binding pocket formed at the IN dimer interface could shift the IN equilibrium toward dimers. We thus tested two peptides, LEDGF(354−378) and its scrambled version LEDGF(353−378 SC), in our IN dimerization assay (Figure 5A). LEDGF(354−378) and LEDGF(354−378 SC) display K_i values of 0.78 μM and 22 μM respectively in our HTRF-based IN−LEDGF interaction assay (*48*). While LEDGF(353−378 SC) displayed a flat dose−response, LEDGF(345−378) displayed a plateau rising to a peak with a subsequent signal decrease to a second potential plateau at high peptide concentrations (Figure 5A). This dose−response can be analyzed phenomenologically by curve fitting using eq II which is the difference between two component equations: an EC_{50} component (red dashed curve) and an IC_{50} component (blue dashed curve) (Figure 5B). We also tested tetraphenyl arsonium chloride (TPAsCl) to determine whether this type of dose−response can be extended to a small molecule that interacts with the IN dimer interface (*53*). TPAsCl competed with LEDGF binding to IN with a K_i value of 167 μM (*48*). TPAsCl displayed the same type of dose−response in the IN dimerization assay as peptide LEDGF(354−378) (Figure 5C). A negative control small molecule that does not interact with IN displayed a flat dose−response curve (Figure 5C).

Analysis of the Dose−Response Curve of IN Dimer Ligands in the IN Dimerization Assay. To understand the unusual shape of the dose−response observed with agents that bind the IN dimer interface, we used Scheme A represented by eq I to simulate the IN dimer ligand dose−response of the sum of heterodimer species ($AB + ABL + ABL_2$) (Figure 6). For

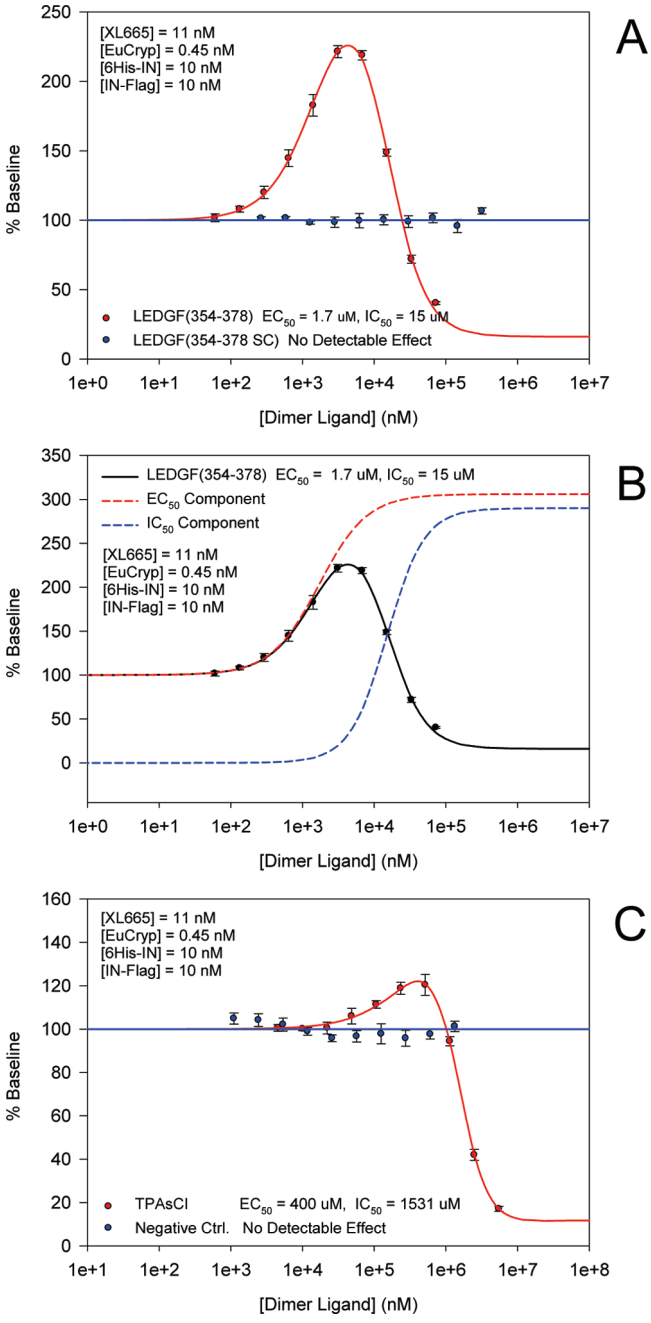

FIGURE 5: Dose−response of IN dimer ligands using the IN dimerization HTRF assay. (A) Dose−response of LEDGF-derived peptide, LEDGF(354−378) and its scrambled counterpart LEDGF(354−378 SC). (B) Phenomenological analysis of a dimer ligand dose−response curve. The dose−response data of the LEDGF-derived peptide, LEDGF(354−378) was fit with eq II (black line). Equation II is the difference between two component equations: an EC_{50} component (red dashed line) and an IC_{50} component (blue dashed line). (C) Dose−response of tetraphenyl arsonium chloride (TPAsCl). The data represent the mean of at least two independent experiments done in quadruplicate with standard deviations shown as error bars. The data are expressed as a percentage relative to the baseline representing the level of all IN heterodimer species in the absence of dimer ligand.

this simulation, we used experimentally determined on- and off-rate constants for IN dimerization (k_{on} = 0.1540 nM^{-1} min^{-1}, k_{off} = 0.0157 min^{-1}), the on- and off-rate constants for an IN dimer ligand (k_{on} = 0.0285 nM^{-1} min^{-1}, k_{off} = 0.2340 min^{-1}), starting IN monomer and dimer equilibrium concentrations for 6His-IN (A) and IN-Flag (B) ($[A]_o = [B]_o$ = 1.82 nM, $[A_2]_o = [B_2]_o$ = 4.09 nM) based on a total concentration of 10 nM for

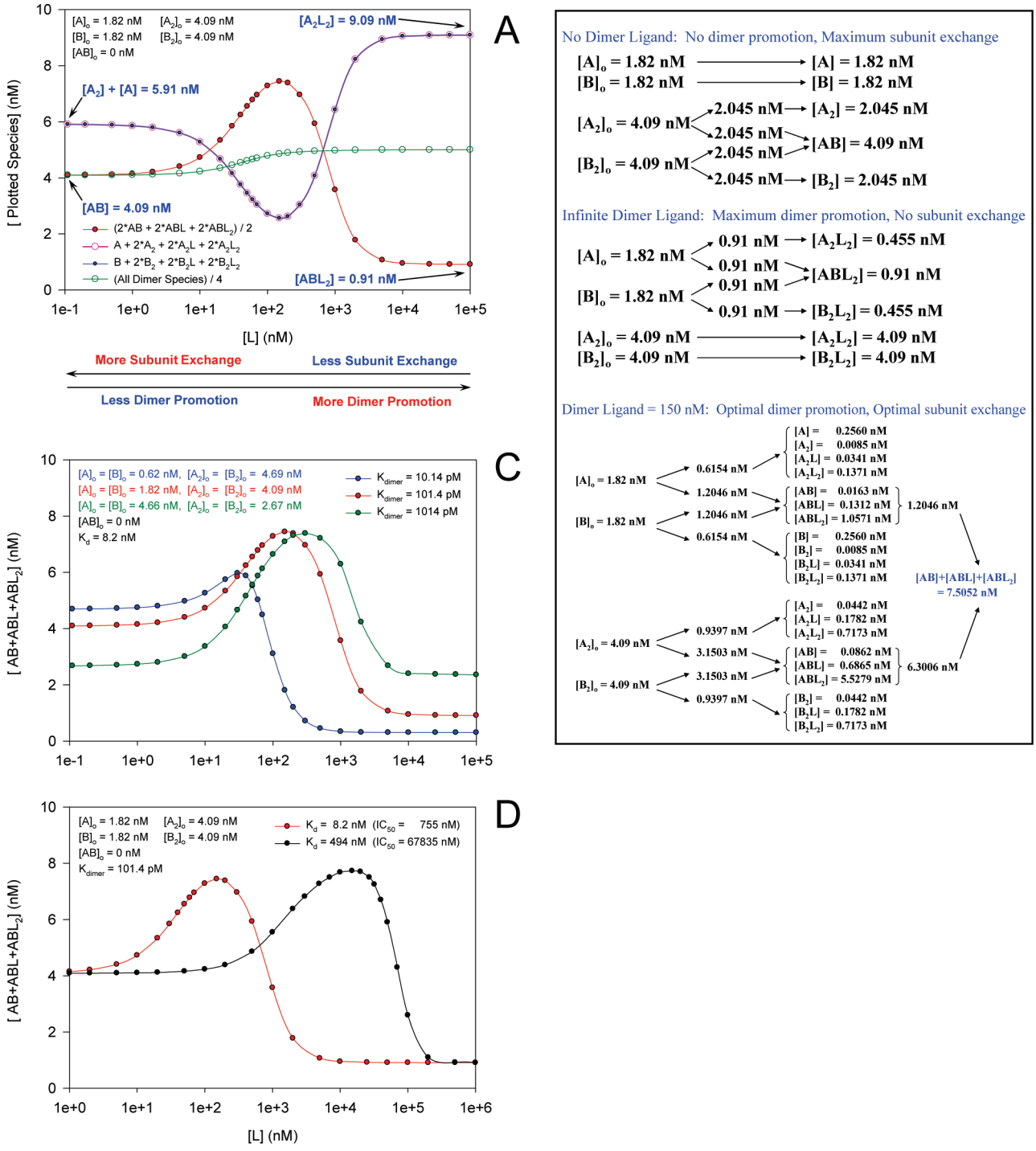

FIGURE 6: Modeling IN dimerization in the presence of an IN dimer ligand. (A) Simulation of dimer ligand, L dose−response. The change in the concentrations of all A species (pink open circle), all B species (blue closed circles), all AB species (red closed circles) and all dimer species (green open circles) were simulated as a function of the concentration of dimer ligand L. All the concentrations are plotted as IN monomer equivalent in (nM). (B) Redistribution of IN monomer and dimer species between the initial and equilibrium conditions. The transition from the initial condition to the equilibrium condition for three concentrations of dimer ligand, $[L]_o$ (0, +∞ and 150) is shown. For $[L]_o$ = 150, initially the total concentration of A is $2[A_2]_o + [A]_o = (2 \times 4.09 + 1.82) = 10$ nM. The total concentration of B is also 10 nM. At equilibrium, the total concentration of A is $[A] + 2[A_2] + 2[A_2L] + 2[A_2L_2] + [AB] + [ABL] + [ABL_2] = 0.2560 + 2(0.0085 + 0.0341 + 0.1371) + 0.0163 + 0.1312 + 1.0571 + 2(0.0442 + 0.1782 + 0.7173) + 0.0862 + 0.6865 + 5.5279 = 10$ nM. The total concentration of B is also 10 nM at equilibrium. The sum of all the heterodimer species is $[AB] + [ABL] + [ABL_2] = 7.5052$ nM at equilibrium and the total dimer ligand, L, bound to integrase at equilibrium is 17.8299 nM. (C) Simulation of all AB species: Dimer ligand dose−response for three different dimer dissociation constants, K_{dimer} (10.14, 101.4, and 1014 pM). (D) Simulation of all AB species: Dimer ligand dose−response for two different affinities of dimer ligand, K_d (8.2 and 494 nM).

each IN species and a dimer dissociation constant of 101.4 pM, and various starting concentrations of dimer ligand L (i.e., 0 to 10000 nM). Simulations showed that the dose−response of the sum of all heterodimeric species (HTRF-detectable species) (Figure 6A, red curve) described a curve that started with a plateau, rose to a peak, and then fell to a second plateau as was observed experimentally with peptide and small molecule IN dimer ligands (Figure 5A,C). Two phenomena are driving signal

formation when A and B are mixed together: (1) dimerization of free monomers A and B to form heterodimer AB and (2) subunit exchange between existing homodimers A_2 and B_2 to form heterodimers AB after dissociation and random reassociation. Addition of an IN dimer ligand, L to the system results in two outcomes: Promotion of overall dimer formation by shifting the equilibrium from monomers to dimers (Figure 6A, green curve) and inhibition of subunit exchange between dimers resulting from their stabilization. Figure 6B illustrates how this system functions under three dimer ligand concentrations (i.e., 0 nM, +∞ nM, and 150 nM, a concentration producing the dose-reponse peak). In the absence of dimer ligand (i.e., $[L]_o = 0$), the proportions of monomers to dimers do not change upon equimolar mixture of the two IN species, maintaining the concentrations of A and B at 1.82 nM at equilibrium. However, the homodimers A_2 and B_2 could exchange their subunits resulting in 2.045 nM each of A_2 and B_2 and 4.09 nM of AB at equilibrium. In the presence of saturating concentrations of IN dimer ligand (i.e., $[L]_o = +\infty$), the ligands will occupy all the binding sites on the IN homodimers and fully block subunit exchange, so that A_2 and B_2, which are fully ligand bound at equilibrium will each remain at their starting concentration of 4.09 nM. In addition, the IN dimer ligands can shift all the free monomers to dimers resulting in 0.455 nM each of additional fully ligand bound A_2 and B_2 and 0.91 nM of fully ligand bound AB heterodimer at equilibrium. These two extreme IN dimer ligand concentrations can explain the two plateaus of the dose−response curve (Figure 6A). A third situation corresponding to the peak shown in Figure 6A (i.e., $[L]_o = 150$) is summarized at the bottom of Figure 6B. Under this condition, all the heterodimer species (i.e., [AB], [ABL], and [ABL_2]) add up to 7.5052 nM giving a peak height of 183.5% (i.e., 7.5052/4.09) measured from the base of the first plateau. On the basis of this model, ligands of IN dimers can promote IN dimerization and inhibit IN subunit exchange. These two effects oppose each other to enable net heterodimer formation. An optimal concentration of IN dimer ligand is required for maximum net heterodimer formation which occurs at the peak of the dose−response. The dose−responses of all A species (Figure 6A, pink curve) and all B species (Figure 6A, blue curve) describe curves that are mirror images of the curve for one-half of all AB species.

To simulate the effect of the IN dimer dissociation constant, K_{dimer} on the dose−response of all AB species, we used three K_{dimer} values with 10-fold increment (10.14, 101.4, and 1014 pM). Each K_{dimer} value resulted in a different starting dimer concentration of 4.69, 4.09, and 2.67 nM respectively for the same total concentration of 10 nM IN (Figure 6C). The simulation showed that the position of the two plateaus depended on the starting concentrations of dimers and monomers (i.e., the more dimers present at the start, the higher the first plateau and the lower the second plateau). It also showed that a smaller K_{dimer} resulted in a smaller peak in the dose−response. Next, we simulated the effect of changing the K_d of dimer ligands (Figure 6D). With larger K_d values, the peak shifted to the right. In the absence of an analytical solution of the dose−response equation for all AB species, we chose to measure the IC_{50} of the descending part of the dose−response curve as a surrogate for estimating the relative affinities of the dimer ligands by curve fitting with eq II (see next section). In the example shown in Figure 6D, the K_d values of 8.2 and 494 nM gave IC_{50} values of 755 nM and 67835 nM, respectively.

The IC_{50} of IN Dimer Subunit Exchange Inhibition Correlates with the K_i for the Disruption of IN−LEDGF

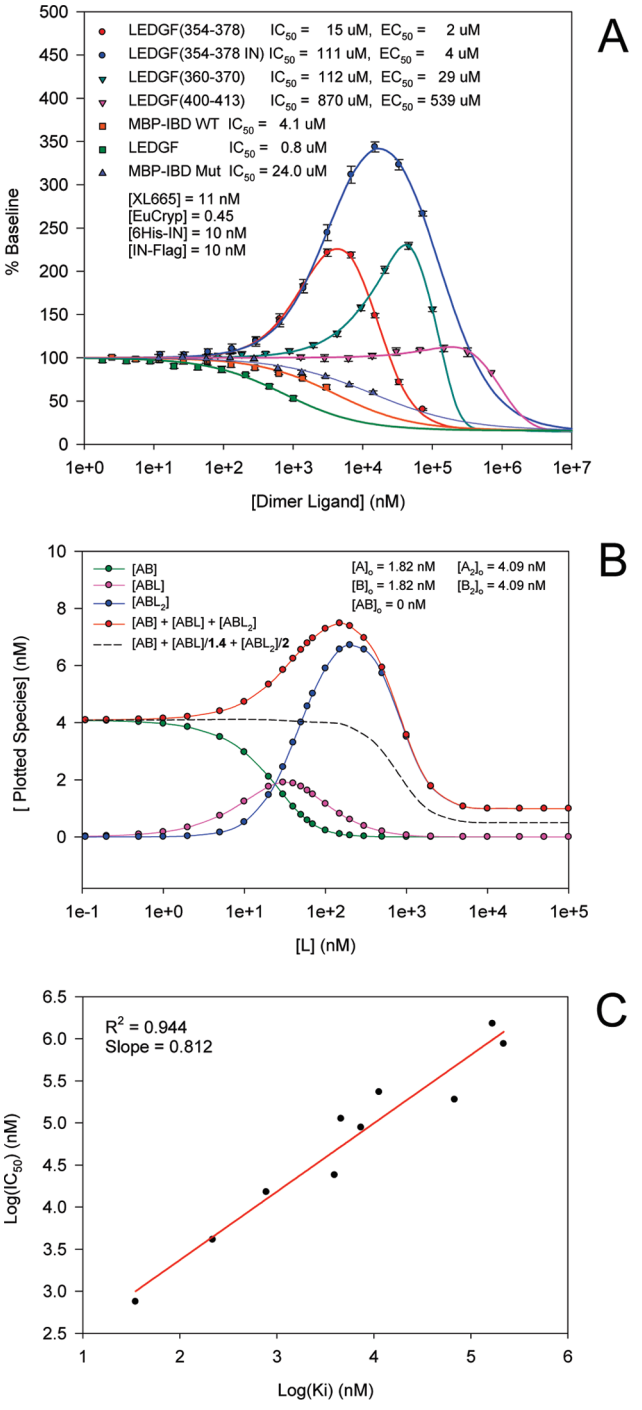

FIGURE 7: Inhibition of IN dimer subunit exchange by dimer ligands and its correlation to competition binding against LEDGF. (A) Dose−response of various IN dimer ligands using the IN dimerization assay. The data represent the mean of two independent experiments done in quadruplicate with standard deviations shown as error bars. The data are expressed as a percentage relative to the baseline representing the level of all IN heterodimer species in the absence of dimer ligand. (B) Simulation of dimer ligand, L dose−response: Effect of partial signal quenching of ABL and ABL_2 species by large ligands. The change in the concentrations of AB species (green circles), ABL species (magenta circles), ABL_2 species (blue circles) and all AB species (red circles) were simulated as a function of the concentration of dimer Ligand L. All the concentrations are plotted as that of the AB heterodimer in (nM). With a 1.4-fold quenching of ABL signal and a 2-fold quenching of ABL_2 signal, the change in the concentration of all AB species will adopted a sigmoidal dose−response (dashed line) in contrast to the unquenched dose response with a peak (red circles). (C) Correlation between the IC_{50} of dimer subunit exchange inhibition and the K_i of competition binding against LEDGF.

Interaction. To assess whether any feature of the dose−response curve (position of peak, EC_{50} or IC_{50}) reflects the affinity of the IN dimer ligand, we tested full-length LEDGF, MBP-IBD and LEDGF-derived peptides in an equilibrium end-point dose−response study using the IN dimerization assay (Figure 7). The peak height of the dose−response curves for different LEDGF-derived peptides was variable which rendered the determination of the peak position difficult. For example, the dose−response curve for LEDGF(400−413) had a very small peak, whereas that of LEDGF(354−378 IN) had a very large peak compared to LEDGF(354−378) and LEDGF(360−370). In contrast, the natural ligands of the IN dimer interface, LEDGF and MBP-IBD displayed only a single inhibition component with no detectable peak in their dose−response curves. According to our simulation (Figure 6C,D), the only parameter that can significantly change the peak height is the dissociation constant of IN dimers, whereas the K_d of the dimer ligand only changes the position of the peak. This variability in peak height was not predicted by our model, which is based purely on the law of mass action and rate constants. However, this result could potentially be explained by taking into consideration properties of macromolecules which may affect fluorescence energy transfer. For large ligands such as LEDGF and MBP-IBD, it is possible that their binding to IN heterodimers could restrict the flexibility of the anti-6His and anti-Flag antibodies and thus prevent Europium Cryptate from coming into close proximity of XL665, thereby reducing the efficiency of FRET. To explore whether such a reduction in FRET could theoretically convert a dose−response curve with a peak to one with a simple sigmoidal shape, we plotted the AB, ABL, and ABL_2 components of the simulated dose−response curve with a K_d of 8.2 nM, which was derived from Figure 6D (Figure 7B). In this simulation, the FRET signal of ligand-bound IN heterodimer species ABL and ABL_2 was reduced by 1.4- and 2-fold, respectively. In this scenario, the sum of all signal generating species described a simple sigmoidal curve (dashed line) instead of a curve with a peak (red line). Because the EC_{50} component was not detectable for some IN dimer ligands, namely, full-length LEDGF and MBP-IBD, we plotted the K_i values of the dimer ligands against the IC_{50} values determined here in the IN dimerization assay. The K_i values were previously determined by competition binding in the IN−LEDGF interaction assay (*48*). The linear correlation between K_i and IC_{50} indicates that the IC_{50} measured in the IN dimerization assay reflects the affinity of dimer ligands for IN (Figure 7C). This IC_{50} also corresponds to the inhibition of IN dimer subunit exchange.

The Rate Constants of IN Dimer Ligands Can Be Determined from the Progress Curve. As noted previously, the variable peak heights produced by the different dimer ligands in conjunction with the difficulty of reaching the high ligand concentrations necessary to obtain a full dose−response for certain ligands represent a hurdle in our data analysis. Therefore, we sought to extract the binding affinities (of IN−IN and IN−ligand interaction) by determining the rate constants from the progress curves of IN dimer subunit exchange in the presence and absence of a dimer ligand. Instead of relying on the equilibrium end point signals at multiple ligand concentrations from a dose−response curve, the on- and off-rate constants of the ligand used at a single concentration can be extracted from the way it alters the real-time kinetics of IN dimer subunit exchange. The variability of peak heights seen with different dimer ligands may be related to differential effects on the FRET efficiency

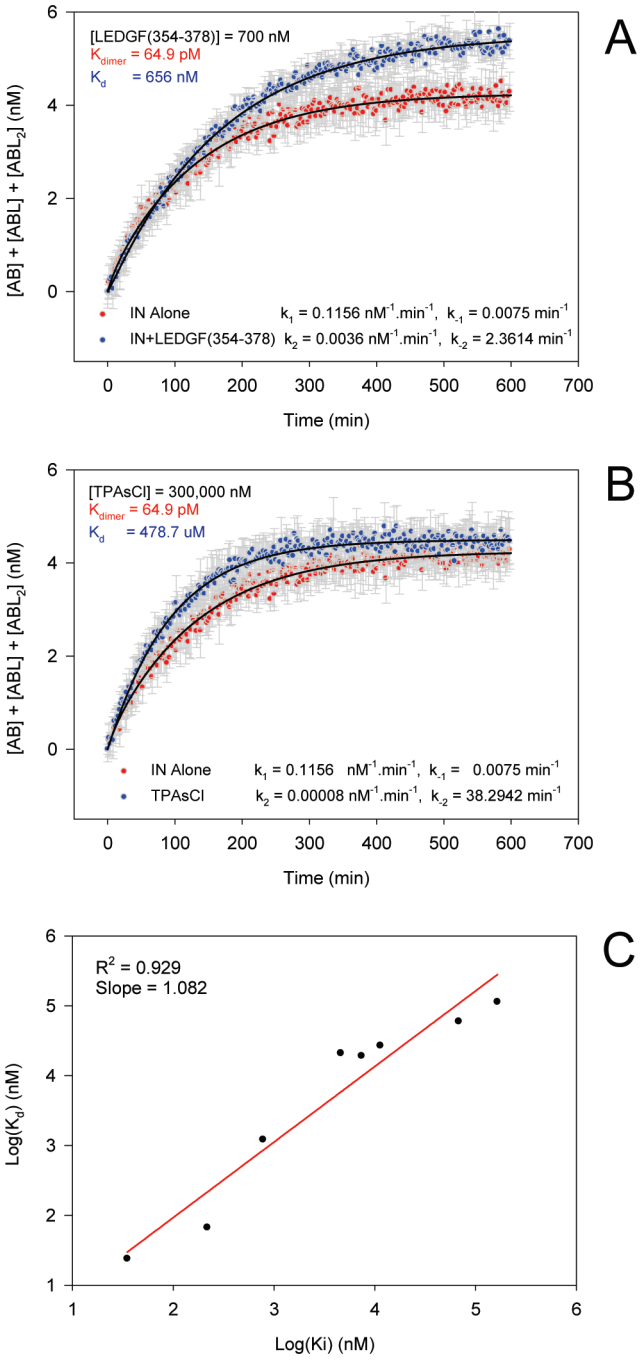

FIGURE 8: Kinetics of IN−IN association in the presence of a dimer ligand. (A) Effect of 700 nM LEDGF(354−378) peptide on the kinetics of IN−IN association. (B) Effect of 300 μM tetraphenyl asornium chloride (TPAsCl) on the kinetics of IN−IN association. Ten nanomolar each of 6His-IN and IN-Flag and a given concentration of dimer ligand each pre-equilibrated separately with both antibody conjugates were mixed and the signal generation was measured for 600 min. The time course was analyzed using Scheme A and eq I where $[A]_o + [A_2]_o = 10$ nM, $[B]_o + [B_2]_o = 10$ nM and $[L]_o = 0$ nM for the no dimer ligand control, 700 nM for LEDGF(354−378) and 300 000 nM for TPAsCl. The on-rate constant (k_1) and off-rate constant (k_{-1}) were first determined for the control without IN dimer ligand by curve fitting using eq I. The on-rate constants (k_2) and off-rate constant (k_{-2}) for the dimer ligand were then determined by substituting k_1 and k_{-1} in eq I with the predetermined values. For both panels A and B, the data represent the mean of hexaplicate runs with standard deviations shown as error bars. The data are expressed as the concentration of all IN heterodimer species in nM. (C) Correlation between the K_d of dimer ligands and their K_i in competition binding against LEDGF.

caused by subtle differences in conformation change upon binding of ligands of different size, shape, and flexibility. This peak height variability should have minimal impact on the rate constants. Figure 8 shows two examples of progress curve alterations, one by 700 nM LEDGF(354−378) (Figure 8A) and the other by 300 μM TPAsCl (Figure 8B). The LEDGF-(354−378) peptide produced an on-rate constant, k_2 of 0.0036 nM^{-1} min^{-1}, which is 45-fold faster than that of TPAsCl and an off-rate constant, k_{-2} of 2.36 min^{-1}, which is 16.2-fold slower than that of TPAsCl, yielding a dissociation constant $K_d = k_{-2}/k_2 = 656$ nM. This dissociation constant for LEDGF(354−378) is comparable to its previously determined K_i of 779 nM in competition binding to IN against LEDGF (*48*). Using the kinetics of IN dimer stablilization, the K_d of several other dimer ligands, including LEDGF-derived peptides, LEDGF, MBP-IBD and small molecule compounds, were also determined. Figure 8C shows that there is good correlation between these K_d values and the K_i values previously determined from competition binding in the IN−LEDGF interaction assay.

DISCUSSION

In this report, we describe a homogeneous time-resolved FRET-based assay of HIV-1 IN dimerization. When coupled with mathematical modeling, this novel assay enabled the study of the dynamic interaction between monomer subunits of HIV-1 IN and how this interaction can be altered by various agents. Using this model system, we discovered that reducing agents, which are necessary for IN strand-transfer activity in vitro, surprisingly promote the dissociation of IN dimers. In contrast, agents that compete with LEDGF binding, by interacting with the LEDGF pocket situated at the IN dimer interface, promote IN dimerization and inhibit IN subunit exchange.

DTT, a reducing agent that is required for HIV-1 IN-mediated strand transfer activity in vitro, produced an intriguing alteration of the competition binding dose−response curves of agents that compete with LEDGF binding to IN. Specifically, DTT induced a peak in the dose−response curve (Figure 1), which is diagnostic of a weakened affinity between IN monomers according to our previously published model of IN-LEDGF interaction (*48*). In this current report, we use a novel IN dimerization assay to demonstrate that DTT and a related reducing agent, β-mercaptoethanol (β-ME), can indeed cause dissociation of IN dimers in a dose dependent manner (Figure 2). When used in kinetic mode, the IN dimerization assay revealed that this disruption of IN dimers by DTT or β-ME did not result from gross unfolding of IN. Instead, these reducing agents caused a decrease in k_{on} and an increase in k_{off}, which resulted in a ∼20-fold increase in the IN K_{dimer} (Figure 4). Importantly, these observations cannot be attributed to disruption of the antiepitope antibodies by the reducing agents (reduction of intermolecular disulfide bonds) since neither DTT nor β-ME altered the ability of the antibody conjugates to bind a peptide that contains the epitopes (Figure 2 and Table 1).

The thiol groups in DTT and β-ME are important for IN dimer disruption since the close analogues threitol and ethylene glycol which contain hydroxyls in place of thiols have no effect on IN dimers (Figure 3). Given the necessity of the thiol groups, we hypothesized that DTT and β-ME could form adducts with the cysteines of IN. However, we find that cysteines 56, 65, 130, and 280 are dispensable for IN dimer dissociation by DTT and β-ME (Figure 4). Reduction of disulfide bridges is not a likely mechanism since IN does not form intra- or intermolecular disulfide bridges between monomer subunits. Formation of an intermolecular disulfide bridge between C280 of IN monomers has been reported in recombinant IN produced in baculovirus infected insect cells, but the C280S mutation did not affect IN activity, oligomerization, or HIV-1 replication (*50*).

Since Zn^{2+} was shown to promote a conformation of IN with enhanced oligomerization (*21*), it was possible that DTT or β-ME reduced the Zn^{2+} in the zinc finger of the N-terminal domain and thus disrupted IN dimers. To explore this hypothesis, we tested the catalytic core domain of IN which is devoid of the NTD and CTD for susceptibility to DTT or β-ME-mediated disruption of dimers. We reasoned that if the zinc finger of the NTD of IN is targeted by DTT or β-ME, then the CCD dimers should be refractory to disruption by these agents. Interestingly, dimers formed by the IN CCD were more susceptible to disruption by DTT or β-ME with IC_{50} values that were significantly lower than those observed with full-length IN (Table 1). While assessing the effect of DTT and β-ME on the association kinetics of INCCD monomers, the rate constants of INCCD dimerization were determined for the first time. The INCCD k_{on} is 0.0072 nM^{-1} min^{-1} and the k_{off} is 0.0039 min^{-1} resulting in a K_{dimer} of 541.7 pM (Figure 4C). Compared to full-length IN monomers, INCCD monomers display a 7.5-fold lower affinity for each other, but INCCD dimers are ∼70- and ∼138-fold more susceptible to DTT and β-ME, respectively. Thus, neither the NTD nor the CTD of IN carries major determinants that confer susceptibility to DTT and β-ME. In fact, deletion of NTD and CTD increased the susceptibility to disruption by DTT and β-ME, suggesting that these domains of IN may mitigate dimer dissociation by these agents. Taken together, these results suggest that none of the cysteine residues in IN are required to observe dimer disruption by DTT and β-ME.

Examination of additional agents revealed that the potency of dimer dissociation is positively correlated to the number of thiol groups. Because thiol-containing agents acted with IC_{50} values in the 1−40 mM range which represents a ratio of ∼0.1−4 million molecules per molecule of IN dimer, it is unlikely that the effect is site-specific. Acetonitrile, a dipolar solvation agent, was reported to dissociate reverse transcriptase heterodimers in a concentration-dependent fashion (*52*). We find that acetonitrile is significantly less potent at causing dissociation of IN dimers compared to reducing agents. The IC_{50} values for acetonitrile in the IN dimerization assay were similar to those observed for RT heterodimer (i.e., in the range of 1000−2000 mM) with a ratios of 100−200 million molecules of the solvent per molecule of IN dimer. This ratio is approximately 2−3 orders of magnitude larger than observed for β-ME and DTT. This larger molar ratio of acetonitrile to IN suggests that the underlying mechanism of IN dimer dissociation by DTT or β-ME is distinct from a solvation mechanism.

Our findings that DTT and β-ME cause dissociation of IN dimers appear at first paradoxical given the well-known fact that DTT stimulates IN activity and is essential for in vitro IN activity assays, while IN multimers are responsible for catalytic activity and tetramers in particular are required for concerted integration (*54*, *55*). Although DTT weakens the interaction between IN monomers, significant affinity between monomers remains (K_{dimer} of ∼1.4−14 nM) at DTT concentrations of 1−10 mM which are commonly used for IN activity assays (*55*−*60*). Our data showed that the optimal DTT concentration for IN strand transfer activity is ∼1.6 mM (Figure S2, Supporting Information).

Evidence that a weakened IN dimer leading to lower multimeric forms may enhance IN function has been provided. For instance, a negative correlation between IN concentration and the efficiency of HIV-1 concerted integration was observed, suggesting that HIV-1 IN must be in a lower multimeric form for optimal interaction with donor DNA (*61*). In addition, preassembled tetramers have been found to be defective for 3′-processing (*39*), again suggesting that lower multimeric forms may favor this catalytic event. The weaker but still substantial affinity between IN monomers in the presence of DTT may thus allow more flexibility in the IN dimer to facilitate assembly with the viral DNA into the fully functional stable synaptic complex. Alternatively, DTT may reduce nonspecific aggregation of IN thus improving enzyme activity.

On the basis of the ability of DTT to weaken IN monomer−monomer interaction, its effect on competition dose−responses in the IN-LEDGF interaction assay and simulations of IN-LEDGF competition dose−response curves, we determined that IN dimers can bind two molecules of LEDGF in our assay system. We used two different binding models to arrive at this conclusion. In the first model, we simulated one LEDGF binding per IN dimer (Figure 9A) and in the second, we simulated two LEDGF molecules binding per IN dimer (Figure 9B). In the one LEDGF per IN dimer model, increasing the K_{dimer} by 6-fold and 18-fold did not alter the shape of the sigmoidal dose−response curve (Figure 9A). In contrast, in the two LEDGF per IN dimer model, the same fold-increase in K_{dimer} changed a sigmoidal dose−response into one with a peak (Figure 9B) which was observed experimentally (Figure 1) and is diagnostic of weakened IN monomer−monomer interactions. The generation of the peak in the two LEDGF per IN dimer model can occur as follows. At low concentrations of LEDGF competitors, the binding of such agents to one of two binding sites on the IN dimer shifts IN equilibrium toward dimers which facilitates the occupation of the second binding site by LEDGF, resulting in a signal increase. At higher LEDGF competitor concentrations, displacement of LEDGF by the competitor would predominate, resulting in a signal decrease. When monomer−monomer interaction is strengthened, the concentration of monomers available for shifting toward dimers by the competitor decreases, resulting in a decreased peak height. If this monomer−monomer interaction is strong enough, the peak will altogether disappear as in the case of IN. An agent that weakens this interaction will have the reverse effect.

In this study, we have expanded our previous model of IN dimerization by incorporating an obligate dimer ligand with two potential binding sites on the IN dimer (Scheme A). This ligand can bind to the LEDGF binding pocket located at the IN dimer interface (*32*) or alternatively to a newly discovered site at the dimer interface adjacent to the LEDGF binding pocket (*62*). Because we now have experimental evidence that an integrase dimer can bind up to two LEDGF molecules in our experimental system, we adopted the two ligand binding model of IN dimerization (Scheme A). Using this model, simulation of IN dimer ligand dose−response of heterodimer formation enabled a detailed understanding of the mechanism underlying the shape of the dose response curves observed with small molecule dimer ligands (Figures 5 and 6). The shape of these dose−responses was characterized by a plateau followed by a peak which then decreases to a second plateau (Figure 5). According to our model, two phenomena are driving IN heterodimer formation. The first is the dimerization of free monomers to form heterodimers and the second is a subunit exchange between existing homodimers after dissociation and random reassociation. With

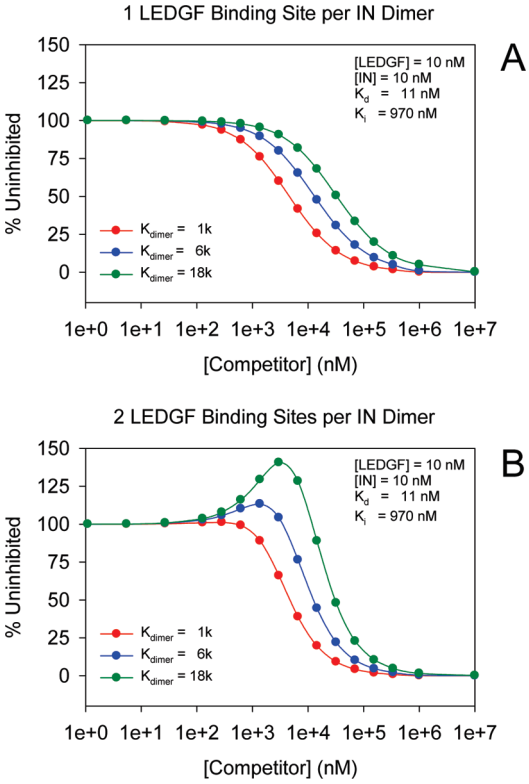

FIGURE 9: Comparison of 1 LEDGF/IN dimer and 2 LEDGF/IN dimer binding models as applied to competition binding against LEDGF. (A) Simulation of competition binding dose−responses using the 1 LEDGF/IN dimer binding model. (B) Simulation of competition binding dose−responses using the 2 LEDGF/IN dimer binding model. These binding models have been previously described (*48*). Simulations in both (A) and (B) were performed using an initial concentration of 10 nM for both IN and LEDGF, a K_d of 11 nM for the IN−LEDGF interaction, a K_i of 970 nM for the competitor, and three hypothetical values of K_{dimer} (1*k*, 6*k* and 18*k* where $k = 14.5$ nM) for the IN−IN interaction.

increasing IN dimer ligand concentration, IN dimer promotion increases whereas IN subunit exchange decreases. Maximum heterodimer formation is enabled at an optimal ligand concentration which defines the peak of the dose response.

We discovered that the IC_{50} of IN subunit exchange in the IN dimerization assay correlated linearly with the K_i values of IN dimer ligands derived from competition binding in the IN-LEDGF interaction assay (Figure 7C) (*48*). This result is consistent with the fact that inhibition of IN subunit exchange and displacement of LEDGF through competition are two manifestations of the same underlying phenomenon, the interaction of these ligands with the LEDGF binding site located at the IN dimer interface. As such, we have established that the IN dimerization assay described in this report can be used as a secondary assay to confirm that a competitor of LEDGF also interacts with the HIV-1 IN dimer. This may be important in drug discovery efforts to discriminate between small molecule inhibitors of the IN−LEDGF interaction that bind to LEDGF from those that bind to IN.

One aspect of the experimental dimer ligand dose−response curves in the IN dimerization assay was not captured by the model in Scheme A which only accounts for signal intensity change as a result of the law of mass action. The model in Scheme A predicted a roughly uniform peak height of ~184% irrespective of the peak position on the ligand concentration axis. The experimental dose−response curves, however, displayed

various peak heights for different ligands and in certain cases exceeding the height of ~184% predicted by the law of mass action (Figure 7A). It has been proposed that a small molecule interacting with the IN dimer inferface may cause slight conformational changes resulting in increased dimer rigidity which in turn could impede the catalytic process (*62*). It is conceivable that various IN dimer ligands may cause different degrees of conformational change to the IN dimer which could in turn alter the distance between the fluorophore donor and acceptor, and thus affect the efficiency of FRET in our IN dimerization assay resulting in different peak heights. This effect on FRET efficiency could result in different peak heights with amplitudes that may be larger or smaller than predicted by the model. The FRET efficiency for each of these complexes [AB], [ABL] and [ABL_2] could be different for a particular ligand. This is evident when the sum [AB] + [ABL] + [ABL_2] being measured in our assay is considered. If the FRET efficiencies for all three AB species were identical, the peak height would be the one predicted by the law of mass action. However, if the FRET efficiencies for [ABL] and [ABL_2] were higher than that of [AB], the peak height would exceed the height predicted by the model.

Dose−response curves generated in the IN dimerization assay with larger IN dimer ligands such as LEDGF or MBP-IBD do not display the peak. To explain this result, we hypothesized that these larger ligands may quench fluorescence energy transfer. By simulating a dose−response curve using different levels of quenching for monoliganded and diliganded IN dimers, we showed that a sigmoidal dose−response curve can be generated through quenching of energy transfer (Figure 7B).

We used the IN dimerization assay in a kinetic mode as an alternate method to assess the affinity of ligands for IN dimers. To achieve this, we analyzed the change in the FRET signal over time instead of the absolute signal at end point. By applying the model in Scheme A to this type of analysis, we were able to determine the k_{on} and k_{off} for various ligands. Interestingly, the K_d of these ligands calculated from the rate constants again displayed a linear correlation with their K_i determined by competition binding in the IN−LEDGF interaction assay (Figure 8C) (*48*).

In this study, we have limited the concentration of IN to 10−20 nM for two reasons. First, the predictive value of a model decreases as its complexity increases. In order to build an IN dimerization/tetramerization model with ligand binding using the two-integrase species (A and B) approach, there would be at least six different unliganded tetramer species to consider. Because there are two high affinity and two low affinity binding sites per tetramer (*40*), for each species of unliganded tetramer, nine additional species of liganded tetramers need to be considered. This would amount to a total of 72 species (i.e., 60 different tetramers species and 12 species of monomers, dimers, and ligand from our current dimerization model with ligand binding) requiring a system of 72 differential equations to be integrated simultaneously. It would be impractical and currently impossible to model tetramerization in addition to dimerization in the presence of ligand in our FRET-based two-integrase species system. This is one experimental reason for operating under conditions where tetramers are negligible so that a relatively simple and elegant model can be applied to derive useful information. Second, integrase has the propensity to aggregate at high concentrations; thus, this FRET-based system cannot be used at integrase concentrations in the triple digit nM range without starting to display large data scatter and signal decreases. To study ligand interaction with IN tetramers would require a different experimental system and a different type of model suited for that system.

Although IN tetramers in the context of the stable synaptic complex are the functional forms of the enzyme capable of concerted integration (*54*, *55*), single IN dimers assembled at individual viral DNA ends are nevertheless capable of 3′-processing and are critical intermediates leading to the formation of the stable synaptic complex (*57*, *59*). Our observation that short LEDGF-derived peptides can promote IN dimer formation beyond what can be accounted for by the law of mass action alone suggests a possible conformational changes in the IN dimer upon binding of these peptides. Such conformational changes in the IN dimer could prevent its correct assembly at the viral DNA ends and thereby inhibit the subsequent steps of integration. In fact, LEDGF-derived peptides very similar to the ones used in our study and small molecules that compete with LEDGF binding to IN inhibit IN activity in both 3′-processing and strand transfer assays (*39*, *44*, *45*, *63*).

The novel methodologies developed in this study should be useful for the characterization of small molecule inhibitors of IN function that interact with the IN dimer interface. They can also be applied to other systems involving obligate dimer binding ligands.

SUPPORTING INFORMATION AVAILABLE

Simulation of integrase heterodimer [AB] and integrase-bound LEDGF ([IN_2L] + 2[IN_2L_2]) as a function of increasing IN dimer dissociation constant K_{dimer} in Figure S1. Effect of DTT on IN strand transfer activity in Figure S2. This material is available free of charge via the Internet at http://pubs.acs.org.

REFERENCES

1. Brown, P. O. (1997) in Retroviruses (Coffin, J. M., Hughes, S. H., Varmus, H. E., Eds.), pp 161−204, Cold Spring Harbor Laboratory, Plainview, NY.
2. Brown, P. O., Bowerman, B., Varmus, H. E., and Bishop, J. M. (1987) Correct integration of retroviral DNA in vitro. *Cell 49*, 347–356.
3. Bowerman, B., Brown, P. O., Bishop, J. M., and Varmus, H. E. (1989) A nucleoprotein complex mediates the integration of retroviral DNA. *Genes Dev. 3*, 469–478.
4. Ellison, V., Abrams, H., Roe, T., Lifson, J., and Brown, P. (1990) Human immunodeficiency virus integration in a cell free system. *J. Virol. 64*, 2711–2715.
5. Farnet, C. M., and Bushman, F. D. (1997) HIV-1 cDNA integration: requirement of HMG I(Y) protein for function of preintegration complexes in vitro. *Cell 88*, 483–492.
6. Bukrinsky, M. I., Sharova, N., McDonald, T. L., Pushkarskaya, T., Tarpley, W. G., and Stevenson, M. (1993) Association of integrase, matrix, and reverse transcriptase antigens of human immunodeficiency virus type 1 with viral nucleic acids following acute infection. *Proc. Natl. Acad. Sci. U. S. A. 90*, 6125–6129.
7. Miller, M. D., Farnet, C. M., and Bushman, F. D. (1997) Human immunodeficiency virus type 1 preintegration complexes: studies of organization and composition. *J. Virol. 71*, 5382–5390.
8. Heinzinger, N. K., Bukrinsky, M. I., Haggerty, S. A., Ragland, A. M., Kewalramani, V., Lee, M. A., Gendelman, H. E., Ratner, L., Stevenson, M., and Emerman, M. (1994) The Vpr protein of human immunodeficiency virus type 1 influences nuclear localization of viral nucleic acids in nondividing host cells. *Proc. Natl. Acad. Sci. U. S. A. 91*, 7311–7315.
9. Lee, M. S., and Craigie, R. (1994) Protection of retroviral DNA from autointegration: involvement of a cellular factor. *Proc. Natl. Acad. Sci. U. S. A. 91*, 9823–9827.
10. Kalpana, G. V., Marmon, S., Wang, W., Crabtree, G. R., and Goff, S. P. (1994) Binding and stimulation of HIV-1 integrase by a human homolog of yeast transcription factor SNF5. *Science 266*, 2002–2006.
11. Chen, H., and Engelman, A. (1998) The barrier-to-autointegration protein is a host factor for HIV type 1 integration. *Proc. Natl. Acad. Sci. U. S. A. 95*, 15270–15274.

12. Yung, E., Sorin, M., Pal, A., Craig, E., Morozov, A., Delattre, O., Kappes, J., Ott, D., and Kalpana, G. V. (2001) Inhibition of HIV-1 virion production by a transdominant mutant of integrase interactor 1. *Nat. Med. 7*, 920–926.
13. Violot, S., Hong, S. S., Rakotobe, D., Petit, C., Gay, B., Moreau, K., Billaud, G., Priet, S., Sire, J., Schwartz, O., Mouscadet, J. F., and Boulanger, P. (2003) The human polycomb group EED protein interacts with the integrase of human immunodeficiency virus type 1. *J. Virol. 77*, 12507–12522.
14. Cherepanov, P., Maertens, G., Proost, P., Devreese, B., Van Beeumen, J., Engelborghs, Y., De Clercq, E., and Debyser, Z. (2003) HIV-1 integrase forms stable tetramers and associates with LEDGF/p75 protein in human cells. *J. Biol. Chem. 278*, 372–381.
15. Maertens, G., Cherepanov, P., Pluymers, W., Busschots, K., De Clercq, E., Debyser, Z., and Engelborghs, Y. (2003) LEDGF/p75 is essential for nuclear and chromosomal targeting HIV-1 integrase in human cells. *J. Biol. Chem. 278*, 33528–33539.
16. Llano, M., Delgado, S., Vanegas, M., and Poeschla, E. M. (2004) Lens epithelium-derived growth factor/p75 prevents proteasomal degradation of HIV-1 integrase. *J. Biol. Chem. 279*, 55570–55577.
17. Llano, M., Vanegas, M., Fregoso, O., Saenz, D., Chung, S., Peretz, M., and Eric M. Poeschla, E. M. (2004) LEDGF/p75 determines cellular trafficking of diverse lentiviral but not murine oncoretroviral integrase proteins and is a component of functional lentiviral preintegration complexes. *J. Virol. 78*, 9524–9537.
18. Bushman, F. D., Engelman, A., Palmer, I., Wingfield, P., and Craigie, R. (1993) Domains of the integrase protein of human immunodeficiency virus type 1 responsible for polynucleotidyl transfer and zinc binding. *Proc. Natl. Acad. Sci. U. S. A. 90*, 3428–3432.
19. Cai, M., Zheng, R., Caffrey, M., Craigie, R., Clore, G. M., and Gronenborn, A. M. (1997) Solution structure of the N-terminal zinc binding domain of HIV-1 integrase. *Nat. Struct. Biol. 4*, 567–577.
20. Zheng, R., Jenkins, T. M., and Craigie, R. (1996) Zinc folds the N-terminal domain of HIV-1 integrase, promotes multimerization, and enhances catalytic activity. *Proc. Natl. Acad. Sci. U. S. A. 93*, 13659–13664.
21. Lee, S. P., Xiao, J., Knutson, J. R., Lewis, M. S., and Han, M. K. (1997) Zn^{2+} promotes the self-association of human immunodeficiency virus type-1 integrase in vitro. *Biochemistry 36*, 173–180.
22. Dyda, F., Hickman, A. B., Jenkins, T. M., Engelman, A., Craigie, R., and Davies, D. R. (1994) Crystal structure of the catalytic domain of HIV-1 integrase: similarity to other polynucleotidyl transferases. *Science 266*, 1981–1986.
23. Goldgur, Y., Dyda, F., Hickman, A. B., Jenkins, T. M., Craigie, R., and Davies, D. R. (1998) Three new structures of the core domain of HIV-1 integrase: an active site that binds magnesium. *Proc. Natl. Acad. Sci. U. S. A. 95*, 9150–9154.
24. Andrake, M. D., and Skalka, A. M. (1995) Multimerization determinants reside in both the catalytic core and C terminus of avian sarcoma virus integrase. *J. Biol. Chem. 270*, 29299–29306.
25. Jenkins, T. M., Engelman, A., Ghirlando, R., and Craigie, R. (1996) A soluble active mutant of HIV-1 integrase: involvement of both the core and carboxyl-terminal domains in multimerization. *J. Biol. Chem. 271*, 7712–7718.
26. Deprez, E., Tauc, P., Leh, H., Mouscadet, J. F., Auclair, C., and Brochon, J. C. (2000) Oligomeric states of the HIV-1 integrase as measured by time-resolved fluorescence anisotropy. *Biochemistry 39*, 9275–9284.
27. Deprez, E., Tauc, P., Leh, H., Mouscadet, J. F., Auclair, C., Hawkins, M. E., and Brochon, J. C. (2001) DNA binding induces dissociation of the multimeric form of HIV-1 integrase: a timeresolved fluorescence anisotropy study. *Proc. Natl Acad. Sci. U. S. A. 98*, 10090–10095.
28. Ciuffi, A., Llano, M., Poeschla, E., Hoffmann, C., Leipzig, J., Shinn, P., Ecker, J., and Bushman, F. (2005) A role for LEDGF/p75 in targeting HIV DNA integration. *Nat. Med. 11*, 1287–1289.
29. Cherepanov, P., Devroe, E., Silver, P. A., and Engelman, A. (2004) Identification of an evolutionarily conserved domain in human lens epithelium-derived growth factor/ transcriptional co-activator p75 (LEDGF/p75) that binds HIV-1 integrase. *J. Biol. Chem. 279*, 48883–48892.
30. Vanegas, M., Llano, M., Delgado, S., Thompson, D., Peretz, M., and Poeschla, E. (2005) Identification of the LEDGF/p75 HIV-1 integrase interaction domain and NLS reveals NLS-independent chromatin tethering. *J. Cell Sci. 118*, 1733–1743.
31. Cherepanov, P., Sun, Z.-Y. J., Rahman, S., Maertens, G., Wagner, G., and Engelman, A. (2005) Solution structure of the HIV-1 integrase-binding domain in LEDGF/p75. *Nat. Struct. Mol. Biol. 12*, 526–532.
32. Cherepanov, P., Ambrosio, A. L. B., Rahman, S., Ellenberger, T., and Engelman, A. (2005) Structural basis for the recognition between HIV-1 integrase and transcriptional coactivator p75. *Proc. Natl. Acad. Sci. U. S. A. 102*, 17308–17313.
33. Hare, S., Shun, M.-C., Gupta, S. S., Valkov, E., Engelman, A., and Cherepanov, P. (2009) A novel co-crystal structure affords the design of gain-of-function lentiviral integrase mutants in the presence of modified PSIP1/LEDGF/p75. *PLoS Pathog. 5*, 1–12.
34. Hare, S., Di Nunzio, F., Labeja, A., Wang, J., Engelman, A., and Cherepanov, P. (2009) Structural basis for functional tetramerization of lentiviral integrase. *PLoS Pathog. 5* (7), e1000515.
35. Emiliani, S., Mousnier, A., Busschots, K., Maroun, M., Van Maele, B., Tempe, D., Vandekerckhove, L., Moisant, F., Ben-Slama, L., Witvrouw, M., Christ, F., Rain, J. C., Dargemont, C., Debyser, Z., and Benarous, R. (2005) Integrase mutants defective for interaction with LEDGF/p75 are impaired in chromosome tethering and HIV-1 replication. *J. Biol. Chem. 280*, 25517–25523.
36. Busschots, K., Voet, A., De Maeyer, M., Rain, J.-C., Emiliani, S., Benarous, R., Desender, L., Debyser, Z., and Christ, F. (2007) Identification of the LEDGF/p75 binding site in HIV-1 integrase. *J. Mol. Biol. 365*, 1480–1492.
37. Rahman, S., Lu, R., Vandegraaff, N., Cherepanov, P., and Engelman, A. (2007) Structure-based mutagenesis of the integrase-LEDGF/p75 interface uncouples a strict correlation between in vitro protein binding and HIV-1 fitness. *Virology 357*, 79–90.
38. Hombrouck, A., De Rijck, J., Hendrix, J., Vandekerckhove, L., Voet, A., Maeyer, M. D., Witvrouw, M., Engelborghs, Y., Christ, F., Gijsbers, R., and Debyser, Z. (2007) Virus evolution reveals an exclusive role for LEDGF/p75 in chromosomal tethering of HIV. *PLoS Pathog. 3*, 418–430.
39. Hayouka, Z., Rosenbluh, J., Levin, A., Loya, S., Lebendiker, M., Veprintsev, D., Kotler, M., Hizi, A., Loyter, A., and Friedler, A. (2007) Inhibiting HIV-1 integrase by shifting its oligomerization equilibrium. *Proc. Natl. Acad. Sci. U. S. A. 104*, 8316–8321.
40. McKee, C. J., Kessl, J. J., Shkriabai, N., Dar, M. J., Engelman, A., and Kvaratskhelia, M. (2008) Dynamic modulation of HIV-1 integrase structure and function by cellular LEDGF protein. *J. Biol. Chem. 283*, 31802–31812.
41. De Rijck, J., Vandekerckhove, L., Gijsbers, R., Hombrouck, A., Hendrix, J., Vercammen, J., Engelborghs, Y., Christ, F., and Zeger Debyser, Z. (2006) Overexpression of the lens epithelium-derived growth factor/p75 integrase binding domain inhibits human immunodeficiency virus replication. *J. Virol. 80*, 11498–11509.
42. Vandekerckhove, L., Christ, F., Van Maele, B., De Rijck, J., Gijsbers, R., Van den Haute, C., Witvrouw, M., and Debyser, Z. (2006) Transient and stable knockdown of the integrase cofactor LEDGF/p75 reveals its role in the replication cycle of human immunodeficiency virus. *J. Virol. 80*, 1886–1896.
43. Llano, M., Saenz, D. T., Meehan, A., Wongthida, P., Peretz, M., Walker, W. H., Teo, W., and Poeschla, E. M. (2006) An Essential Role for LEDGF/p75 in HIV Integration. *Science 314*, 461–464.
44. Al-Mawsawi, L. Q., Christ, F., Dayama, R., Debyser, Z., and Neamati, N. (2008) Inhibitory profile of a LEDGF/p75 peptide against HIV-1 integrase: Insight into integrase−DNA complex formation and catalysis. *FEBS Lett. 582*, 1425–1430.
45. Hou, Y., McGuinness, D. E., Prongay, A. J., Feld, B., Ingravallo, P., Ogert, R. A., Lunn, C. A., and Howe, J. A. (2008) Screening for antiviral inhibitors of the HIV integrase-LEDGF/p75 interaction using the AlphaScreen luminescent proximity assay. *J. Biomol. Screen 13*, 406–414.
46. Debyser, Z. Cellular co-factors of HIV integrase − from target identification to drug discovery. Abstr. 16th Conference on Retroviruses and Opportunistic Infections, Montreal, Canada, 2009, abstr. 74, p 91.
47. De Luca, L., Barreca, M. L., Ferro, S., Christ, F., Iraci, N., Gitto, R., Monforte, A. M., Debyser, Z., and Chimirri, A. (2009) Pharmacophore-based discovery of small-molecule inhibitors of protein-protein interactions between HIV-1 integrase and cellular cofactor LEDGF/p75. *ChemMedChem 4*, 1311–1316.
48. Tsiang, M., Jones, G. S., Hung, M., Mukund, S., Han, B., Liu, X., Babaoglu, K., Lansdon, E., Chen, X., Todd, J., Cai, T., Pagratis, N., Sakowicz, R., and Geleziunas, R. (2009) Affinities between the binding partners of the HIV-1 integrase dimer/ lens epithelium derived growth factor (IN dimer/LEDGF) complex. *J. Biol. Chem. 284*, 33580–33599.
49. Christ, F., Voet, A., Marchand, A., Nicolet, S., Desimmie, B. A., Marchand, D., Bardiot, D., Van der Veken, N. J., Van Remoortel, B., Strelkov, S. V., De Maeyer, M., Chaltin, P., and Debyser, Z. (2010) Rational design of small-molecule inhibitors of the LEDGF/p75-integrase interaction and HIV replication. *Nat. Chem. Biol. 6*, 442–448.

50. Bischerour, J., Leh, H., Deprez, E., Brochon, J.-C., and Mouscadet, J.-F. (2003) Disulfide-linked integrase oligomers involving C280 residues are formed in vitro and in vivo but are not essential for human immunodeficiency virus replication. *J. Virol. 77*, 135–141.
51. Zhu, K., Dobard, C., and Chow, S. A. (2004) Requirement for integrase during reverse transcription of human immunodeficiency virus type 1 and the effect of cysteine mutations of integrase on its interactions with reverse transcriptase. *J. Virol. 78*, 5045–5055.
52. Divita, G., Restle, T., and Goody, R. S. (1993) Characterization of the dimerization process of HIV-1 reverse transcriptase heterodimer using intrinsic protein fluorescence. *FEBS Lett. 324*, 153–158.
53. Molteni, V., Greenwald, J., Rhodes, D., Hwang, Y., Kwiatkowski, W., Bushman, F. D., Siegel, J. S., and Choe, S. (2001) Identification of a small-molecule binding site at the dimer interface of the HIV integrase catalytic domain. *Acta Crystallogr. D57*, 536–544.
54. Faure, A., Calmels, C., Desjobert, C., Castroviejo, M., Caumont-Sarcos, A., Tarrago-Litvak, L., Litvak, S., and Parissi, V. (2005) HIV-1 integrase crosslinked oligomers are active *in vitro*. *Nucleic Acids Res. 33*, 977–986.
55. Li, M., Mizuuchi, M., Burke, T. R., Jr., and Craigie, R. (2006) Retroviral DNA integration: reaction pathway and critical intermediates. *EMBO J. 25*, 1295–1304.
56. Li, M., and Craigie, R. (2005) Processing of viral DNA ends channels the HIV-1 integration reaction to concerted integration. *J. Biol. Chem. 280*, 29334–29339.
57. Guiot, E., Carayon, K., Delelis, O., Simon, F., Tauc, P., Zubin, E., Gottikh, M., Mouscadet, J. F., Brochon, J. C., and Deprez, E. (2006) Relationship between the oligomeric status of HIV-1 integrase on DNA enzymatic activity. *J. Biol. Chem. 281*, 22707–22719.
58. Yu, F., Jones, G. S., Hung, M., Wagner, A. H., Macarthur, H. L., Liu, X., Leavitt, S., McDermott, M. J., and Tsiang, M. (2007) HIV-1 integrase preassembled on donor DNA is refractory to activity stimulation by LEDGF/p75. *Biochemistry 46*, 2899–2908.
59. Lesbats, P., Metifiot, M., Calmels, C., Baranova, S., Nevinsky, G., Andreola, M. L., and Parissi, V. (2008) In vitro initial attachment of HIV-1 integrase to viral ends: control of the DNA specific interaction by the oligomerization state. *Nucleic Acids Res. 36*, 7043–7058.
60. Valkov, E., Gupta, S. S., Hare, S., Helander, A., Roversi, P., McClure, M., and Cherepanov, P. (2009) Functional and structural characterization of the integrase from the prototype foamy virus. *Nucleic Acids Res. 37*, 243–255.
61. Sinha, S., and Grandgenett, D. P. (2005) Recombinant human immunodeficiency virus type 1 integrase exhibits a capacity for full-site integration in vitro that is comparable to that of purified preintegration complexes from virus-infected cells. *J. Virol. 79*, 8208–8216.
62. Kessl, J. J., Eidahl, J. O., Shkriabai, N., Zhao, Z., McKee, C. J., Hess, S., Burke, T. R., Jr., and Kvaratskhelia, M. (2009) An allosteric mechanism for inhibiting HIV-1 integrase with a small molecule. *Mol. Pharmacol. 76*, 824–832.
63. Hayouka, Z., Levin, A., Maes, M., Hadas, E., Shalev, D. E., Volsky, D. J., Loyter, A., and Friedler, A. (2010) Mechanism of action of the HIV-1 integrase inhibitory peptide LEDGF 361−370. *Biochem. Biophys. Res. Commun. 394*, 260–265.